We are IntechOpen, the world's leading publisher of Open Access books
Built by scientists, for scientists

4,800
Open access books available

122,000
International authors and editors

135M
Downloads

Our authors are among the

154
Countries delivered to

TOP 1%
most cited scientists

12.2%
Contributors from top 500 universities

CLARIVATE ANALYTICS
BOOK CITATION INDEX
INDEXED

WEB OF SCIENCE™

Selection of our books indexed in the Book Citation Index in Web of Science™ Core Collection (BKCI)

Interested in publishing with us?
Contact book.department@intechopen.com

Numbers displayed above are based on latest data collected.
For more information visit www.intechopen.com

Chapter

Designing a Tunnel

Spiros Massinas

Abstract

Designing a tunnel is always a challenge. For shallow tunnels under cities due to the presence of buildings, bridges, important avenues, antiquities, etc. at the surface and other infrastructures in the vicinity of underground tunnels, parameters like vibrations and ground settlements must be tightly controlled. Urban tunnels are often made in soils with very low values of overburden. Risks of collapse and large deformations at the surface are high; thus negative impact on old buildings are likely to occur if appropriate measures are not taken in advance, when designing and constructing the tunnel. For deep tunnels with high overburden and low rock mass properties, squeezing conditions and excessive loads around the excavation can jeopardize the stability of the tunnel, leading to extensive collapse. The aim of the chapter is to give details on advance computational modelling and analytical methodologies, which can be used in order to design shallow and deep tunnels and to present real case studies from around the world, from very shallow tunnels in India with only 4.5 m overburden to a deep tunnel in Venezuela with extreme squeezing conditions under 1300 m overburden.

Keywords: tunnel, shallow tunnelling, deep tunnels, surface settlements, tunnel squeezing, analytic solution, numerical analysis, lining stress controllers, sliding joints, monument underpassing, monitoring, plasticity, TBM, earth pressure balance shield, high overburden, high deformations, NATM, conventional tunnelling

1. Introduction

The aim of the current chapter is to give details and guidance in designing underground tunnels, to be constructed with tunnel boring machines (TBM).

In the sequence of paragraphs to follow, the reader will get a grasp of tunnelling principles and theory related to mountainous and urban tunnelling—deep and shallow tunnels will be explained (paragraph 2).

In paragraph 3, details for designing mechanized constructed (TBM) Metro tunnels in urban environment will be given, and real cases from India will be presented. Special case for monument underpass with earth pressure balance machine (EPBM) under extreme low overburden will also be discussed, and the real case study from Chandpole Gate in Jaipur will be presented.

Mountainous and deep tunnels design will be presented in paragraph 4. Squeezing and non-squeezing conditions will be explained, and methods of designing will be given, along with examples from around the world.

The final paragraph will summarize the primary conclusions from the presented design methodologies. It is noted that all the examples presented herein are real cases of tunnels already constructed, with the personal involvement of the author in their designs elaboration.

2. Tunnelling principles

Tunnelling is divided in two general categories: the deep tunnel case and the shallow tunnel case (**Figure 1**). The most common example of a shallow tunnel is the Metro Lines in a big city. For example, underground tunnels realize the connection between the underground stations. Since the stations are constructed, as underground structures, to serve the surface mass transit system, the depth of the train platform from the surface is limited to meters; in a normal typical station, the platform depth can vary from 15 to 25 m, while for other cases like flagship stations connecting different Metro Lines, platforms can be in different levels, and consequently their depth can reach and even exceed 40 m. Therefore, the tunnels connecting the stations can also vary in depth, and the typical overburden height (distance between the tunnel crown and the surface) can be 10–20 m, while for deeper sections can reach or even exceed 35 m. Of course along a Metro Line, there are always unique cases where the tunnel depth can be very limited, and thus the overburden height can be even less than a tunnel diameter (e.g., 5 m); for such a special case, the real case study from Chandpole Gate in Jaipur will be presented in the following paragraphs. Therefore, from a mathematical perspective, in shallow tunnelling, two boundaries are introduced, the tunnel geometry (circular or not) and the surface (**Figure 1**).

On the contrary, for a deep tunnel case, the problem can be described only by one boundary, the tunnel geometry (**Figure 1**). Furthermore, the influence of the variation of the in situ stress with the depth is more intense and critical in a shallow tunnel rather than in a deeper tunnel case. In the latter, the in situ stress difference between tunnel crown and invert is insignificant compared to the absolute value of the in situ stress at this depth. To understand the main difference between shallow and deep tunnel, a characteristic example of a motorway with multiple tunnels crossing a mountainous terrain can be used. In such a case where the tunnel pierces a mountain, the overburden height can be decades of meters (120, 150 m, etc.) or even hundreds of meters and even can exceed 1000 m; a real case study for a very deep tunnel in Venezuela will be presented later on.

The first to differentiate the shallow from the deep tunnel, covering, also, the intermediate zone between deep and shallow tunnels, was Bray [2]. In order to do so, he introduced the dimensionless ratio of the depth (from tunnel center—di) to the radius (ri) of a tunnel. For a ratio (di/ri) equal or greater to 25—e.g., a tunnel with radius 5 and 120 m overburden height—the deep tunnel case is described, while the shallow tunnel is defined by a ratio (di/ri) smaller or equal to 7—e.g., a

Figure 1.
Shallow and deep tunnels [1].

tunnel with radius 5 and 25 m overburden. For the intermediate values of the ratio, thus between 7 and 25, a transition zone is defined. The stress distribution around an underground cavity either shallow or deep is the key factor to design a tunnel.

In a similar fashion to the lines of flow in the current of a river, which are deviated by the pier of a bridge and increase in speed as they run around it, the flow lines of the stress field in a rock mass are deviated by the opening of a cavity (tunnel) and are channelled around it to create a zone of increased stress around the walls of the excavation. The channelling of the flow of stresses around the cavity introduces the arch effect (**Figure 2**).

Arch effect can occur, depending on the size of the stresses (overburden height) and the geomechanical properties of the rock mass (strength and deformation properties), (a) close to the profile of the tunnel, (b) far from the profile of the tunnel, and (c) not at all.

Case (a) occurs when the rock mass around the tunnel withstands the deviated stress flow, responding elastically in terms of strength and deformation. In case (b), due to the low properties of the rock mass, the ground around the excavation is not able to withstand the deviated stress flow and thus responds nonelastically, plasticizing and deforming in proportion to the volume of ground involved in the plasticization phenomenon. The latter, that often causes an increase in the volume of the ground affected, propagates radially and deviates the channelling of the stresses outwards into the rock mass until the triaxial stress state is compatible with the strength properties of the rock mass. In this situation, the arch effect is formed far from the line of the excavation and the ground around the tunnel which has been plasticized (plastic zone), contributing to the final tunnel stability with its own residual strength giving rise to deformations, which is often sufficient to compromise the safety of the excavation. With proper support measures, the ground can be "helped"; the plasticization phenomena can be limited, and thus the formation of the arch effect by natural means can be produced, and the tunnel stability can be ensured. In the third case (c), the ground around the cavity is completely unable to withstand the deviated stress flow and responds in the failure range producing the collapse of the tunnel. In such case the arch effect cannot be formed naturally, and thus pre-support measures must be used before the excavation, in order artificially to initiate the arch effect.

The reaction is the deformation response of the medium (ground) to the action of excavation (tunnelling). It is always generated ahead of the excavation face within the area that is disturbed, following the generation of greater stress in the medium around the cavity. The deformation response always depends on the

Figure 2.
Flow lines in the current of a river around a pier (left) and stress field flow lines around a tunnel [1].

medium's properties and its stress state and is affected by the tunnel's face advance. As the face advances, the tunnel passes from a triaxial to a plane stress state. In case that the progressive decrease in the confinement pressure at the face ($\sigma_3 = 0$) produces stress in the elastic range ahead of the face, then the excavation face remains stable with limited and absolutely negligible deformation. In this case the channelling of stresses around the cavity (arch effect) is produced by natural means close to the profile of the excavation, and no artificial support is required to secure the tunnel stability. If, on the other hand, the progressive decrease in the stress state at the face ($\sigma_3 = 0$) produces stress in the elastoplastic range ahead of the face, then elastic-plastic deformation of the face will give rise to a condition of short-term stability. This means that in the absence of any intervention, plasticization is triggered, which, by propagating radially and longitudinally from the walls of the excavation, produces a shift of the "arch effect" away from the tunnel further into the rock mass. This shift from the theoretical profile of the tunnel can only be controlled by intervention to stabilize the ground.

Therefore, in respect to the in situ ground properties, the in situ stress field, and the applied support measures/pressure, the stress redistribution remains within the elastic domain, or a phenomenon of plasticization is triggered which may result to the formation of a plastic domain around the tunnel. Extent/width and shape of the plastic zone around the cavity are the main parameters for calculating/evaluating the stability conditions of an underground excavation. The impact of this mechanism is different in a shallow and a deep tunnel.

In a shallow tunnel, the overburden height is limited. Therefore, any underground deformation that may result from the soil plasticization will affect the development of the surface settlements. In case that the extent of the plastic zone gives rise to excessive surface settlements (**Figure 3**), damages on the surface structures can also be significant or even severe. For a shallow tunnel design, the key parameter is to minimize the magnitude of the developed surface settlements, and thus the redistribution of the stresses around the tunnel needs to be controlled accordingly by designing and applying proper support measures and consequently proper support pressure (Pi). However, for the deep tunnel case the redistribution of the stresses around the excavation can be the main challenge. The increased overburden height combined with low ground mass properties can give rise to excessive loads exerted around the excavation and thus can lead to tunnel collapse, if non-proper design of the support measures is elaborated. In such difficult cases, safe tunnel advance can only be achieved with controlled plasticization of the

Figure 3.
Impact of plastic zone formation around a shallow (left) and a deep (right) tunnel.

groundmass; intervening with application of proper yielding support measures if the groundmass is deformed plastically under controllable manner, and thus the exerted loads can significantly be reduced.

Three main different methods can be applied to solve tunnelling problems:

a. Analytic

b. Computational

c. Combination of the above

Analytic methods are related with the use of closed form solutions, while the finite element method (FEM) and the finite difference method (FDM) describe the computational procedures. Finally, combination of closed form solutions with FEM or FDM modelling can be more beneficial than the other two methods along; closed form solution can give the opportunity to the designer for quick and accurate calculations and thus to be properly "guided" in the elaboration of the final FEM/FDM modelling. Indeed, empirical methods (e.g., Protodiakonov, Terzaghi, etc.) are also used in some cases for solving tunnelling problems.

3. TBM shallow tunnelling in urban environment

The principle objective when designing a shallow tunnel in an urban environment is to minimize the induced surface settlements. Therefore, the face stability along with the tunnel's induced displacements are the key factors to control the extent of the plastic zone formation and consequently to secure the surface structures from undesirable settlements. In order to design the tunnel, the method of construction to be adopted for the work's execution needs to be defined. In the current paragraph, the principles for designing a Metro tunnel constructed with tunnel boring shield machine (earth pressure balance (EPB)-TBM) will be discussed, and the main design phases will be explained in detail.

After the alignment is fixed, the geological and geotechnical conditions along the alignment of a Metro project are always the main input required in order to further design the tunnels. Knowledge of the regional geology of the area along with geotechnical investigation campaign is always mandatory in order to determine the ground properties (**Figure 4**).

Boreholes with sampling, executed typically every 50–150 m, aim to investigate the ground conditions at least one to two diameters below the tunnel invert.

Mainly the complexity of the geological model of the area is a key factor to determine the required number of the boreholes along the alignment and if additional investigations such as geophysical surveys will be needed. For example, for the phase 3 of Delhi Metro, the general geology of the area (**Figure 4**) reveals the existence of polycyclic sequence of brown silty clay with kankar, fine- to medium-grained micaceous sand, c-silty/clay, and s-sandy facies. Those thick layers of alluvium deposits mainly are known as Delhi Silt with almost uniform properties along the alignment. Indeed, the presence of quartzite rock is also visible in certain areas of Delhi. Although the exposures are very less in number, structurally it occurs in the form of anticline and syncline with axial trend as N-S and SE-NW; their appearance within the tunnel excavation face (mainly consisted of soft soil—Delhi silt) can be detrimental for the tunnel construction with TBM. Therefore, geotechnical campaign with dense boreholes were executed (varying from 50 to 70 m distances) with the aim to investigate

IntechOpen

IntechOpen

Figure 4.
Geological map of Delhi (Source: Geological Survey of India) (Delhi Metro Phase 3 area marked with blue circle).

the actual depth of the bedrock (**Figure 5**), to quantify the risk from having mixed face conditions (soft soil with hard rock), and finally to determine the arrangement of the EPB-TBM cutterhead (to be designed for mixed face conditions) (**Figure 6**).

For another case, where the stratigraphy is uniform along the entire alignment, the boreholes can be in greater distance. Let us investigate another example, again from India but from another area, the state of Rajasthan and the Jaipur Metro Phase 1B.

Figure 5.
Geological longitudinal section of shallow tunnel in Delhi Metro Phase 3 (CC23), with boreholes [3]—Delhi silt marked with yellow color and quartzite rock with magenta.

Figure 6.
EPB-TBM cutterhead designed by Herrenknecht for mixed face conditions. Cutter discs are visible (Delhi Metro Phase 3—CC23). Source: FEMC-Pratibha JV.

Quaternary sediment occupies the major northeastern part of Jaipur, but hillocks and ridge are present around the city (**Figure 7**). Granite gneisses occupy the southern part of the district. Other important lithological unites exposed in Jaipur are limestone, sandstone, etc. Soil alluvium is the main formation along the alignment of the project, in the form of sand to silty sand with gravels. The uniformity on the geological conditions dictated the determination of a geotechnical campaign with boreholes in greater distances varying from 100 to 150 m (**Figure 8**).

On the contrary to the Delhi Metro, the EPB-TBM for Jaipur is designed with an open spoke-type cutterhead with opening ratio of 60%, suitable for the sandy formations (**Figure 9**). The increased opening ratio of the cutterhead is more suitable in applying uniformly the earth pressure on the excavation face but is essential to maintain always the pressure in every stroke of the machine as it moves forward, in order to avoid face instabilities and excessive surface settlements.

For both cases, Delhi and Jaipur Metro, the water table is revealed below the tunnel invert.

3.1 Geotechnical assessment and interpretation

Following the geotechnical campaign and the laboratory tests on the samples, which are taken from the executed boreholes, the geotechnical model will be determined along with the characteristic geotechnical parameters of the soil formations. The modulus of elasticity (E), the effective cohesion (c′), effective friction angle (φ′ or phi), and the unit weight (γ) of the soil formations are the main geomechanical properties required for designing the tunnel excavation. While the effective cohesion and friction angle are critical parameters that will govern the extent of the plastic zone shape, the modulus of elasticity controls the magnitude of the surface settlements, and the tunnel depth is the geometrical parameter that will affect the shape of the surface settlement trough.

When tunnelling with EPB shields, the surface settlement development is related with the machine operation in conjunction with the soil properties. The so-called volume loss, resulted from the face extrusion (face loss), the steering gap closure (radial loss on the shield), and the annular void between the segmental lining and the soil, are basic key parameters that will affect the magnitude of the soil's deformations. It is obvious that the soil properties are the governing factors for determining the operation parameters of the TBM, in order to keep the volume loss within acceptable limits, to control the plastic zone formation, and thus to minimize the surface settlements.

Since the tunnel excavation with EPB shields is a short-term procedure, the properties of the soil should be addressed in a careful manner in order to describe the actual geotechnical conditions. Continuous support on the tunnel face is applied by using the freshly excavated soil, which completely fills up the work chamber (muck). The supporting pressure is achieved through control of the incoming and outgoing materials in the chamber, i.e., through regulation of the screw conveyor rotation speed and of the excavation advance rate.

Underestimation of the mechanical characteristics of the soil medium and especially underestimation of the modulus of elasticity E can lead to the calculation of unreasonable and extremely high values of support pressure, with detrimental effect on the operation of the machine, as demonstrated below:

a. The muck exhibits a shear resistance that, for a given internal friction angle, increases with the support pressure. Since muck with shear resistance does not behave like a fluid, the stress field in the work chamber, and thus the distribution of the support pressure along the tunnel face, is not under control (**Figure 10a**).

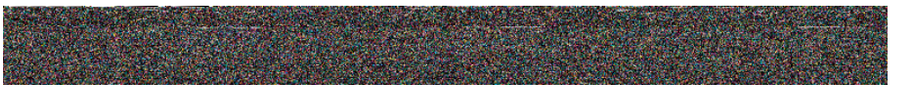

Figure 7.
Geological map of greater area of Jaipur—Rajasthan (Source—Geological Survey of India) (Jaipur Metro Phase 1B area marked with magenta circle).

DOI: http://dx.doi.org/10.5772/intechopen.90182

Figure 8.
Geological longitudinal section of shallow tunnel in Jaipur Metro Phase 1B, with boreholes [4]—Silty sand along the entire alignment marked with orange color.

Figure 9.
EPB-TBM open spoke-type cutterhead designed by Robbins for sand and silty sand (Jaipur Metro Phase 1B).

IntechOpen

IntechOpen

Figure 10.
Typical problems caused by high support pressure in EPB shields.

This is a nonoptimal situation from a stability point of view. The problem of nonuniform distribution of support pressure becomes even worse in the case of a mixed tunnel face due to the widely differing stiffnesses of the rock and soil layers.

b. For a full work chamber, the cutting wheel not only separates the ground from the tunnel face but also shears the compacted muck during the rotation. The larger the support pressures in the work chamber, the larger the shear resistance that must be overcome (**Figure 10b**). Thus, larger support pressures result in greater torque and in excessive cutterwear.

c. For high support pressures and low clay percentages, arching of the muck occurs at the entrance to the screw conveyor and inhibits further discharge. In case that the excavation continues with impeded discharge, the muck becomes further compacted. It will be obvious that a silty, sandy soil is especially susceptible to arching and that the cutting wheel could then be brought to a complete halt due to the very high necessary torque (**Figure 10c**).

Conservatism in determining the geotechnical properties of the soil not only can result in overdesigning the permanent segmental lining of the tunnel but also can lead to unreasonably high support pressures with immediate detrimental effect on the operation of the machine. Furthermore, for very shallow tunnel cases, the blowout is also a case that needs to be carefully studied before determining the final EPB support pressure.

For soft soil formations, modulus of elasticity can be evaluated on the basis of the SPT results and the respective uncorrected N_{60} value, as per CIRIA report 143. Based on this report, the consistency of soils is determined by SPT N values as illustrated in **Table 1**.

Cohesionless soils		**Cohesive soils**	
SPT N (uncorrected value)	**Classification**	**SPT N (uncorrected value)**	**Classification**
0–4	Very loose	0–4	Very soft
4–10	Loose	4–8	Soft
10–30	Medium	8–15	Firm
30–50	Dense	15–30	Stiff
>50	Very dense	30–60	Very stiff
>60	Hard	>60	Hard

Table 1.
Consistency of soil formation based on SPT N values as per CIRIA, R143.

Figure 11.
Characteristic plots showing the variation on SPT N value with depth along the tunnel alignment. Delhi Metro (CC23), left plot; Jaipur Metro Phase 1B, right plot.

In order to establish the representative SPT N_{60} values along the tunnel, the respective values should be plotted versus depth for the entire alignment considering the results from all the boreholes (**Figure 11**).

Further plots can also be prepared for different stretches, e.g., considering the boreholes results of the same stretch (between two stations). With this approach the entire tunnel stretch can be divided in sub-areas, and different fit lines can be determined as linear equations linking the representative N value with depth (e.g., N = 2.8z + 5, whereas z = depth below ground surface). Therefore, by considering the CIRIA report, the modulus of elasticity can be calculated versus the SPT N_{60} values. As an example, for silts, sandy silts, and silty sands, the equation E = 0.7–1.0 N_{60} can determine the modulus of elasticity. For the derivation of the cohesion and friction angle, consolidated undrained triaxial strength tests (CU) when possible and direct shear strength tests can be used.

As already mentioned, underestimation of the soil properties when calculating the EPB pressure can lead to excessive problems during construction of the tunnel. Therefore, it is essential to study in detail the soil behavior not only through the results of the laboratory tests but also by investigating physical exposed open cuts in order to understand the "stand-up time" of the formations. "Stand-up time" is the short-term stability of the soil without the application of support measures and mainly reveals the existence of increased shear strength on the formation which sometimes is difficult to be determined by laboratory tests.

As a conclusive remark, it is worth mentioning that when designing the excavation of a tunnel with shield machine, it is proper to use the upper values of the soil parameters, while when designing the permanent lining, lower values can be used with caution to avoid unnecessary overdesign.

3.2 EPB-TBM principles

The tunnel boring machines that provide immediate peripheral and frontal support simultaneously belong to the closed-face group. They excavate and support both the tunnel walls and the face at the same time. Except for mechanical support machines, they all have the, so-called, cutterhead chamber at the front, separated by the remaining part of the machine by a bulkhead, where a confinement pressure is maintained in order to actively support the excavation and/or balance the hydrostatic pressure of the groundwater. The TBM is moving forward through hydraulic cylinders that are pushing the already erected segmental lining (**Figure 12**). Respective video for the operation of an EPB can be found in the following link from Herrenknecht: https://www.herrenknecht.com/en/products/productdetail/epb-shield/.

DOI: http://dx.doi.org/10.5772/intechopen.90182

Figure 12.
Typical view of earth pressure balance (EPB) shield (Source: Herrenknecht).

With earth pressure balance shields, the cohesive soil loosened by the cutting wheel serves to support the tunnel face, unlike other shields which are dependent on a secondary support medium (e.g., slurry shields). The area of the shield in which the cutting wheel rotates is known as the excavation chamber and is separated from the section of the shield under atmospheric pressure by the pressure bulkhead. The soil is loosened by the cutters on the cutting wheel, falls through the openings of the cutting wheel into the excavation chamber, and mixes with the plastic soil already there. Uncontrolled penetration of the soil from the tunnel face into the excavation chamber is prevented because the force of the thrust cylinders is transmitted from the pressure bulkhead onto the soil. A state of equilibrium is reached when the soil in the excavation chamber cannot be compacted any further by the native earth and water pressure. The excavated material is removed from the excavation chamber by an auger conveyor (screw of Archimedes). The amount of material removed is controlled by the speed of the auger and the cross section of the opening of the upper auger conveyor driver. The auger conveyor conveys the excavated material to the first of a series of conveyor belts. The excavated material is conveyed on these belts to the so-called reversible conveyor from which the transportation gantries in the backup areas are loaded when the conveyor belt is put into reverse. The tunnels are normally lined with steel- or fiber-reinforced lining segments, which are positioned under atmospheric pressure conditions by means of erectors in the area of the shield behind the pressure bulkhead and then temporarily bolted in place. Mortar is continuously forced into the remaining gap between the segments' outer side and the rock through injection openings in the tailskin or openings directly in the segments.

The principle of EPB-TBM operation is that pressurizing the spoil held in the cutterhead chamber to balance the earth pressure exerted holds up the excavation. If necessary, the bulkhead spoil can be made more plastic by injecting additives from the openings in the cutterhead chamber, the pressure bulkhead, and the muck-extraction screw conveyor. By reducing friction, the additives reduce the torque required to churn the spoil, thus liberating more torque to work on the face. They also help maintain a constant confinement pressure at the face. The hydrostatic pressure is withstanding by forming a plug of confined earth in the chamber and screw conveyor; the pressure gradient between the face and the spoil discharge point is balanced by pressure losses in the extraction and pressure relief device (**Figure 13**).

Face support is uniform. It is obtained by means of the excavated spoil and additives. Injecting products through the shield can enhance additional peripheral support. For manual work to proceed in the cutterhead chamber, it may be necessary to create a sealing cake at the face through controlled substitution (without loss of confinement pressure) of the spoil in the chamber with bentonite slurry. The architecture of this type of TBM allows for rapid changeover from closed mode to open mode operation and vice versa. The tunnel lining is erected inside the TBM tail skin, with a tail skin seal, ensuring there are no leaks. Back grout is injected behind the lining as the TBM advances.

IntechOpen

Figure 13.
Earth pressure balance principle (Source: Herrenknecht).

Following the EPB operation principles, it is obvious that the tunnelling-induced soil movements can occur at the longitudinal and radial direction. The face extrusion can give rise to longitudinal displacements, while the gap around the shield and the tail of the machine will introduce radial convergence. The volume of soil that intrudes into the tunnel owing to the pressure release at the excavated face will be excavated eventually. This movement of soil is defined as the volume of material that has been excavated in excess of the theoretical design volume of excavation and is called "ground loss" or "volume loss." Therefore the volume loss for a tunnel excavated with TBM occurs in three stages:

- Face loss (longitudinal ground movement into the tunnel face)
- Shield loss (radial ground movement into the gap created by the TBM overcut)
- Tail loss (due to the gap closure at the tail).

IntechOpen

Since the above ground losses are related with the cavity displacements, consequently this is the mechanism that will give rise to the development of the surface settlements. Designing a TBM tunnel means control of the volume loss, and this can be achieved with:

- Proper calculation and application of face support
- The earth pressure support that is applied at the tunnel face is also transferred to the shield gap (thus around the shield), through the cutterhead openings, and therefore reduces the shield's radial displacements
- Injecting products (e.g., bentonite) through the shield openings can also enhance additional peripheral support
- Tail skin grouting to seal the gap between erected segments and the tunnel's excavated profile will minimize the so-called development of secondary settlements

DOI: http://dx.doi.org/10.5772/intechopen.90182

IntechOpen

IntechOpen

Figure 14.
Overview of a TBM tunnel interstation design.

3.3 TBM tunnel interstation design (TID)

Following the finalization of the ground design parameters, documented in the Geotechnical Interpretation Report (GIR), the design for the excavation and support of the tunnel with the TBM will follow and is called TBM tunnel interstation design. The scope of the TBM TID is the complete tunnel boring design in order to ensure, the safety of the tunnel structure itself, the surface and subsurface structures adjacent to the project and, finally, the confinement of the ground deformations within permissible limits. A TBM TID (**Figure 14**) is divided in the following parts:

- Calculation of the required TBM support pressure. The required support pressure per ring, to be applied by the EPB-TBM on the excavation face and consequently around the shield gap, which is produced due to the overcut.
- Calculation of the ground surface settlements contours within the influence zone of the tunnelling works.
- Risk assessment of the existing structures due to tunnelling works, through different staged analysis (stage 1–3).
- Determination of protection measures for existing structures, if required according to the results from the staged analysis.

According to the analysis methodology that is related with the control of the induced surface settlements, the following basic phases are considered in a TBM TID:

i. *Evaluation phase*: At the current stage, the geotechnical-geomechanical design parameters of the different formations need to be examined and evaluated, which are the input data for describing the initial conditions of the problem. All the above are always given in the Geotechnical Interpretation Report.

ii. *Diagnostic phase*: The tunnel face and cavity behavior is examined along the tunnel alignment for different overburden heights, since the face and cavity stability affects the development of the ground displacements and hence the induced surface settlements. Therefore in a TID, three different categories need to be considered in order to describe the excavation face reaction:

   - Category 1: "Stable," elastic behavior
   - Category 2: "Stable for limited time," elastic-plastic behavior with limited plastic zone width
   - Category 3: "Unstable," elastic-plastic behavior with extended plastic zone width

Two categories to describe the deformation phenomena:

- Elastic
- Elastoplastic

And finally two categories to describe the cavity behavior:

- Stable

- Unstable

iii. *Therapy phase*: According to the results derived from the previous phase (II), the required parameters (e.g., support pressure, TBM operation parameters) are determined in order to secure the face and cavity stability and thus to minimize the induced surface settlements.

After studying the tunnel alignment, the designer will define the critical sections of the project, which is a combination of ground properties, water table height, overburden height, axial distance between the two tunnel bores (in cases of twin bore tunnels), locations of the existing buildings, and important structures. The outcome of the study will determine the tunnel sections of the TID. In detail the characteristic tunnel sections that need to be used in a TID will include mainly the following cases:

- Section with the highest overburden
- Section with the shallowest overburden
- Section with the highest (expected) groundwater table
- Section with the lowest (expected) groundwater table
- Section with the highest loading acting on the ground surface
- Section with possible non-horizontal ground surface
- Section in which existing buildings or important structures exist
- Section in which adjacent present or future tunnel exists
- Section that includes the existence of possible future works (expect of tunnels)
- Sections with any changing geometry or geology

During the tunnel excavation, the development of the surface settlements will be recorded through an established geomechanical monitoring program, in order to check the predictions of the TID and to calibrate if required the operation parameters of the EPB machines (e.g., support pressure).

3.3.1 Part A: face pressure calculation

The tunnel face and cavity reaction is always related with the following main key parameters:

- Ground mass geotechnical properties and water table level. "Output" of the GIR
- The overburden thickness. Determined based on the tunnel's alignment
- Tunnel radius. Defined by the project's requirements
- Tunnel construction methodology

Section	Overburden (m)	Ground condition	Water table	Existing structures above tunnel
F1	25	Delhi silt	Nil	≤5-storey
F2	22	Delhi silt	Nil	≤5-storey
F3	19	Delhi silt	Nil	≤5-storey
F4	17	Delhi silt	Nil	≤5-storey
F5	15	Delhi silt	Nil	≤5-storey
F6	13	Delhi silt	Nil	≤5-storey
F7	12	Delhi silt	Nil	≤5-storey
F8	11	Delhi silt	Nil	≤5-storey
U1	4.5	Delhi silt	Nil	Existing Metro Line-2 with tunnel invert 4.5 m above tunnel crown of CC23
U2	3.8	Delhi silt	At surface	Existing bridge and "Nala" (water canal) with bridge's foundation level 3.8 m above tunnel crown

Table 2.
Critical sections along CC23 of Delhi Metro Phase 3.

Section	Overburden (m)	Ground condition	Water table	Existing structures above tunnel
J1	7	Silty sand	Nil	Roadway
J2	10	Silty sand	Nil	Roadway
J3	12	Silty sand	Nil	Roadway
CH	4.5	Silty sand	Nil	Chandpole Gate with foundation level 4.5 m above tunnel crown

Table 3.
Critical sections along Jaipur Metro Phase 1b.

For the determination of the required support pressure, different calculation sections are required to be defined as explained in the previous paragraph. To present the design methodology in more detail, the Delhi Metro Phase 3 and Jaipur Metro Phase 1b will be used as case studies hereafter.

Considering the geological longitudinal section of the contract CC23 of Delhi Metro Phase 3, snapshot of it presented in **Figure 5**, the critical sections defined along the entire alignment are given in **Table 2**.

Considering now the geological longitudinal section of the Jaipur Metro Phase 1b, snapshot of it presented in **Figure 8**, the critical sections defined along the entire alignment are given in **Table 3**.

For all sections of **Tables 2** and **3**, where the tunnel alignment is below roadway and buildings with less or equal to 5 storeys, a uniform surface load of 50 kPa is considered. This approach is common when designing shallow tunnels in urban environment, since a minimum surface load is always required in order to consider any unforeseen load case or any low height (<5 storeys) future structure. Sections U1, U2, and CH are the most critical cases, since the existing structures are in very close proximity with the tunnel crown; thus special considerations will be presented hereafter.

The geomechanical parameters of the soils for the abovementioned Metro projects (Delhi and Jaipur) are also given in **Table 4**.

Design parameter	**CC23 Delhi Metro Phase 3**		**Jaipur Metro Phase 1b**	
Characteristic N_{60} value	2.8z + 5, z = depth below ground surface (m)		3.2z + 5, z = depth below ground surface (m)	
Modulus of elasticity, E [MPa]	1.0 × N_{60}		1.0 × N_{60}	
Effective friction angle, φ′ [°]	Depth 0–15 m	30	Depth 0–10 m	27
	Depth 15–25 m	32	Depth >10 m	30
	Depth 25–>30 m	34		
Effective cohesion, c′ [kPa]	Depth 0–7.5 m	0	Depth 0–>25 m	5
	Depth 7.5–15 m	10		
	Depth 15–25 m	20		
	Depth 25–>30 m	30		
Unit weight, γ [kN/m^3]	20		19	
Coefficient of earth pressure at rest, K_o	0.61		0.57	
Poisson's ration, v	0.3		0.4	

Table 4.
Geotechnical design parameters.

Figure 15.
CC23 Delhi Metro. Calculation of plastic zone width according to Massinas and Sakellariou solution [6] for different tunnel depths (as per sections of **Table 2***). Proposed range of support pressure also shaded with orange color.*

According to the international literature and case studies from various projects around the world, the applied support pressure for the tunnel construction with TBM shields is considered according to the earth pressure at rest and active earth pressure or according to Anagnostou and Kovari [5]. Recently, the Massinas and Sakellariou [6] analytic solution is also used to determine the required support pressure for EPB

IntechOpen

Figure 16.
CC23 Delhi Metro. Calculated EPB support pressure for different overburden heights as per the critical sections F1–F8 of **Table 2**. *Pressures P_r and P_a are calculated based on earth pressure at rest and active earth pressure, respectively. P_{sm} (min) and (max) give the range of calculated support pressure based on Massinas and Sakellariou closed form solution [6].*

shields [7, 8]). Considering the geotechnical parameters of the soil, the Massinas and Sakellariou solution [6] is used to calculate the min and max value of the support pressure (**Figure 15**). The proposed range of pressure, given by Massinas and Sakellariou, coincides with minimum plastic zone width (less than 0.5–1 m). Since the aim is to minimize the induced surface settlements, controlling the plastic zone formation to minimum width can determine the required value of support pressure.

Considering also earth pressure at rest (K_o) and active (K_a), the EPB support pressure is calculated for all the different sections F1–F8 of **Table 2**, for CC23 Delhi Metro. All the calculation results are plotted in the diagram of **Figure 16**.

It is obvious that the calculation of P_r by considering the earth pressure at rest leads to non-pragmatic values, not feasible for the tunnel construction. On the other hand, the active earth pressure seems to give more realistic results since P_a is almost coincide with the upper values of the pressures range, as calculated according to Massinas and Sakellariou solution. Most realistic results can be derived by Massinas and Sakellariou analytic solution; since the soil-tunnel-surface interaction is considered and the plastic zone width is derived, therefore the proposed support pressure to be applied by the EPB is concluded, and the input for part B is defined. More details for the application of Massinas and Sakellariou method can be found in Refs. [6–8].

For the special case U1, the bored tunnels of CC23 (Line-8) underpass the existing tunnels of Line-2 as shown in **Figure 17**. The objective of securing the safe operation of the existing Metro Line-2 is related with the reduction of the soil deformations and thus minimizing the displacement of the existing segmental lining. In order to examine the soil-structure interaction by calculating the plastic zone formation around the tunnel and calculating the EPB support pressure (P_{sm}) range, again the method of Massinas and Sakellariou needs to be applied, with the assumptions that follow.

The presence of the existing Line-2 is taken into consideration by assuming as an upper boundary of the semi-infinite space its invert foundation level; thus a total overburden of 4 m (conservatively instead of 4.5 m) is considered, to examine the interaction between the new and the existing tunnel (**Figure 18**—left); the total earth pressure (due to gravity) at the real depth of the tunnel is taken into account, by applying a uniform load (Po) at the upper boundary of the half-space.

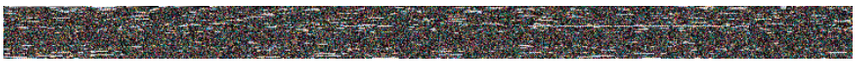

Figure 17.
CC23 Delhi Metro. Key plan and typical cross section of Line-8 bored tunnels under existing Metro tunnels of Line-2 [6, 7].

Figure 18.
CC23 Delhi Metro. Physical and analytical model for calculating the required support pressure of Line-8 TBM under the existing Metro tunnels of Line-2 (left). Analytic calculation of plastic zone width (right) [6, 7].

By using the analytic solution formula [6], the calculation of the plastic zone shape around the tunnel is performed for different values of the support pressure (**Figure 18**—right). Minimum plastic zone of less than 0.5 m is derived for support pressure range of 1.8–2.2 bar, while for 2.4 bar, the soil around the cavity remains within the elastic domain. Therefore by considering a support pressure within the range of 1.8–2.2 bar, the stress redistribution remains within the elastic domain, and thus minimum displacements are expected to be developed. The above-derived conclusion is the initial observation for the tunnel interactions and is further analyzed (part B of TID) in full detail through 3D elastic-plastic FDM multistaged simulations with powerful software Fast Lagrangian Analysis of Continua in 3 Dimensions (FLAC3D) [9].

For the second special case U2 of CC23 Line-8, the TBM working on the up line underpass the existing Nala, while for the construction of the down line, the TBM will underpass both the abutments of the existing bridge as well as the Nala. Therefore, the critical area is approximately 50 m, starting from the neutral zone (cut and cover structure). Typical plan view of the horizontal alignment and the longitudinal sections of the down line tunnel is given in **Figure 19**.

Special survey on the bridge's foundation (trial pit) revealed pad foundation with thickness of approximately 2.33 m. The bridge is new, and the span is approx. 26 m with general dimensions in plan 35 × 14 m (length × width). The superstructure is made of prestressed reinforced concrete box and lay on the abutments through bearings, as presented in **Figure 20**.

As in the previous case U1, also for this critical section U2, the presence of the existing bridge is considered by assuming as an upper boundary of the semi-infinite space its foundation level; thus a total overburden of 4 m is considered, to examine the interaction between the bridge and the tunnel. Furthermore, the total earth pressure (due to gravity) at the real depth of the tunnel is also taken into account, and a total uniform load (P_o) at the upper boundary of the half-space is applied (**Figure 20**—right). Considering the longitudinal section of the tunnel, different overburden heights are considered for the analytic calculations in order to determine the required support pressure. **Table 5** summarizes the calculated support pressure as per TID—part A for different overburden heights along the bridge and Nala area.

For the calculation of P_{sm} pressures, the same principle, as in previous case U1, is used. Thus, the required pressure is calculated in order to keep the plastic zone width around the tunnel below 0.5 m. As per part B of TID, further analysis of the

Figure 19.
CC23 Delhi Metro Line-8. Horizontal alignment (left) of up and down lines in Nala (water canal) area. Longitudinal section (right) of down line shows tunnel under the bridge abutments and the Nala [10].

Figure 20.
CC23 Delhi Metro Line-8. Cross section of Line-8 tunnels under existing bridge (left). Physical and analytical model for calculating the required support pressure of Line-8 TBM under the existing bridge (right) [10].

Pressure	11 m overburden (bar)	8 m overburden (bar)	Bridge location (bar)	Nala deepest part (bar)
P_r (at rest)	1.7	1.3 bar	2.3 bar	1.0 bar
P_a (active)	0.9	0.7	1.3	0.5
P_{sm} (Massinas and Sakellariou)	1.0–1.2	0.8–1.0	1.5–1.7	0.6–0.8
Adopted pressure for part C of TID	1.0	1.0	1.5	1.0

Table 5.
Support pressure along tunnel alignment, for different overburden heights.

settlement development is required to be elaborated through 3D calculations with FLAC3D [9], considering the different support pressures given in **Table 5**.

For the case of Jaipur Metro Phase 1b, the critical section is more complex than in previous examples from Delhi Metro. The importance of the monument of Chandpole Gate and the extremely shallow depth of the tunnels (**Figure 21**) required further study to determine the most appropriate method for underpassing with the TBM.

For the determination of the structure's foundation system, dimensions and condition, special survey was carried out, consisting of nine trial pits that were executed in certain locations near the Gate. According to the findings from the trial pits on both sides of the structure, the Gate rests on stone masonry foundation with depth of approx. 2.0–2.4 m, whereas below the main arch, a boulder layer was found with depth ~1.5 m near the Gate's walls and ~1.0 m below the mid part. Water pipes and other utilities were found below the two passageways and the main arch. A typical section of the Gate with its foundations and the underpassing TBM tunnels is given in **Figure 21** (right), indicating the soil cover of approx. 4.5 m between the bottom of the Gate's foundation and the tunnels' crown.

Examination and co-evaluation of the geotechnical investigation and Gate foundation survey results was jointly performed by the designer and the contractor, aiming to decide on the necessity of soil strengthening through grouting below and around the Gate's foundation. The grain size distribution of the in situ soil practically excluded the successful and efficient application of low-pressure cement grouting, even with use of microfine cement. Other grouting methods that would be more appropriate for this soil type, e.g., jet grouting and compensation grouting, were excluded, as the risk of soil disturbance, instability, temporary liquefaction, and settlement below the Gate foundation was considered too high for

Figure 21.
Jaipur Metro Phase 1b. Horizontal alignment and typical cross section of TBM tunnels under Chandpole Gate [8].

Figure 22.
Jaipur Metro Phase 1b. Physical and analytical model for TBM support pressure calculation under Chandpole Gate (left). Analytic calculation of plastic zone width (right) [8].

Section	Overburden (m)	Ground condition	Adopted support pressure (bar)	Settlement analysis method
F1	25	Delhi silt	1.5	3D FDM with FLAC3D
F2	22	Delhi silt	1.4	3D FDM with FLAC3D
F3	19	Delhi silt	1.2	3D FDM with FLAC3D
F4	17	Delhi silt	1.1	3D FDM with FLAC3D
F5	15	Delhi silt	1.0	3D FDM with FLAC3D
F6	13	Delhi silt	0.8	3D FDM with FLAC3D
F7	12	Delhi silt	0.8	3D FDM with FLAC3D
F8	11	Delhi silt	0.8	3D FDM with FLAC3D
U1	24/4.5	Delhi silt	1.8	3D FDM with FLAC3D
U2	11	Delhi silt	1.0	3D FDM with FLAC3D
	8	Delhi silt	1.0	3D FDM with FLAC3D
	Bridge	Delhi silt	1.5	3D FDM with FLAC3D
	Nala	Delhi silt	1.0	3D FDM with FLAC3D

Table 6.
Critical sections along CC23 of Delhi Metro Phase 3 with proposed support pressure for settlement analysis.

the significance and vulnerability of the structure. Additionally, the loading of the structure itself and the long period of its application was naturally assumed to have made the soil below the Gate compact. This assumption could be partly verified by the soil inspection in the trial pits. In the light of the above considerations, the designer and the contractor decided to underpass the structure without any pre-treatment of the soil, relying on the appropriate TBM operation, mainly in terms of applied face pressure and annular gap grouting application.

Following the same procedure as for the Delhi Metro cases, the presence of the existing Gate was considered by assuming its foundation level as an upper boundary of the semi-infinite space. Thus a total overburden of 4.5 m has been considered to examine the interaction between the Gate and the tunnel, as presented in **Figure 22**. Furthermore, the total earth pressure (due to gravity) at the real depth

Section	Overburden (m)	Ground condition	Adopted support pressure (bar)	Settlement analysis method
J1	7	Silty sand	1.1	3D FDM with FLAC3D
J2	10	Silty sand	1.4	3D FDM with FLAC3D
J3	12	Silty sand	1.5	3D FDM with FLAC3D
CH	Chandpole Gate/4.5	Silty sand	1.5	3D FDM with FLAC3D

Table 7.
Critical sections along Jaipur Metro Phase 1b with proposed support pressure for settlement analysis.

of the tunnel is also considered, and a total uniform load (P_o) at the upper boundary of the half-space is applied. The comparison between the physical model of the problem and its equivalent model for the analytical calculations is illustrated in **Figure 22** along with the results derived by the application of Massinas and Sakellariou analytic solution.

A minimum plastic zone width (<0.5 m) is calculated for a mean support pressure within the range of 1.4–1.5 bar, while for 1.6 bar, the soil around the excavation remains within the elastic domain. The value of 1.5 bar was selected for the execution of 3D numerical analyses for settlement prediction.

To summarize the results from part A of TID, **Tables 6** and 7 give the final proposed TBM support pressures used for the settlement analysis in part B of TID.

For all the above cases as summarized in **Tables 6** and 7, the adopted support pressure for the settlements analysis is based on the calculation results as per Massinas and Sakellariou solution [6]. Comparing the two tables, it is obvious that for the case of Jaipur Metro Phase 1b, higher pressures are considered, which resulted from the requirement to keep the plastic zone width around the tunnel less than 0.5 m since the entire tunnel alignment is very shallow (7–12 m) compared to CC23 Delhi Metro.

Furthermore, even along the Jaipur Metro Phase 1b, the tunnel alignment is below the busy roadway; in close vicinity with the tunnel's sides, the very old buildings of the "Pink City" and other important monuments exist (**Figure 23**), and thus the settlement needs to be kept to absolute minimum values to avoid any damages.

3.3.2 Part B: surface settlements

Following the derivation of the support pressures in part A, settlement analysis is required in part B of TID in order to numerically calibrate the range of the derived support pressures. The outcome form this step of the design will finalize the set of values to be used during construction that will result to minimum volume loss and consequently will reduce the magnitude of the surface settlements. Since the

Figure 23.
Jaipur Metro Phase 1b. Important monuments of the "Pink City" along the tunnel alignment [12].

"geometric constraints" of the problem is bounded with the construction sequence of the tunnel (excavation-segment installation-grouting) that takes place near the face, the most effective type of analysis in order to investigate the face behavior and the cavity convergence around the shield is to perform 3D calculations.

Assuming stress-induced failure mode of ground mass, the computational three-dimensional analysis is performed with a continuum model approach, using the finite difference software FLAC3D [9]. In order to ensure the accuracy of the results and to avoid any "boundary effects," certain parametric 3D analyses are performed (benchmark tests) with different 3D meshes in dimension and density. In all vertical boundaries, the horizontal movements normal to the boundary were restricted. On the bottom boundary, soil movements were restricted in all directions. In order to avoid any effects on the surface settlements shape and magnitude, due to boundary positions, the proper grid dimensions were implemented in the models. Thus, for the vertical boundaries on each side of the tunnels, a distance of 10 x diameters is selected. For the extension of the grid below the tunnel spring line, a distance of 2 x diameters is considered. The distance between the vertical boundary normal to the tunnel direction in front of tunnel's face and the final excavation face is selected equal to 10 x diameters [13]. Typical views of the models are presented in **Figure 24**.

For the special cases U1, U2, and CH, different models were constructed following the same boundary conditions and dimensions as presented before. For the underpass of Yellow Line (U1), both the existing Line-2 and the Hauz Khas station (in close vicinity with the tunnels) were simulated (**Figure 25**).

Figure 24.
Typical FDM models used for settlement analysis. CC23 Delhi Metro on the left and Jaipur Metro Phase 1b on the right [11, 12].

Figure 25.
Section U1: underpass of Line-2. Typical FDM model used for the settlement analysis. CC23 Delhi Metro [14].

DOI: http://dx.doi.org/10.5772/intechopen.90182

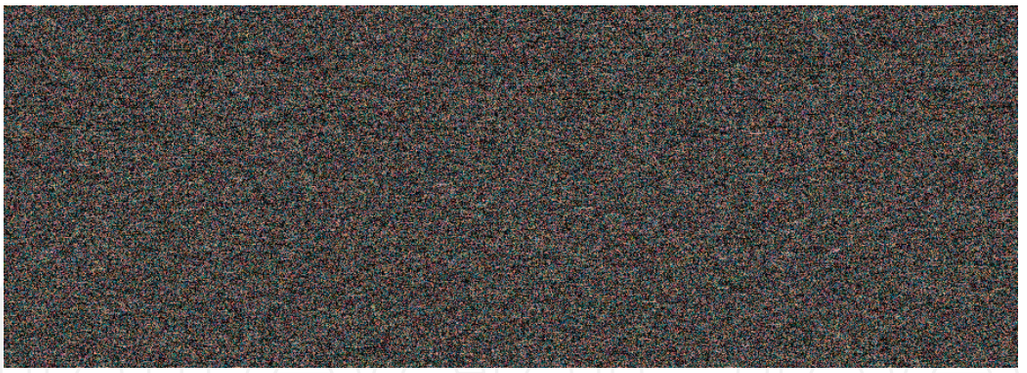

Figure 26.
Section U2: underpass of bridge and Nala. Typical FDM model used for the settlement analysis (left). Additional support measures for soil strengthening under the bridge's abutment (right). CC23 Delhi Metro [10].

Figure 27.
Section CH: underpass of Chandpole Gate. Typical FDM model used for the settlement analysis. Jaipur Metro Phase 1b [15].

For the settlement analysis at bridge and Nala area (U2), the 3D model considered the cut and cover structure of the neutral station the bridge's foundation. The anaglyph of the Nala with the physical slopes is also detailed simulated (**Figure 26**). Due to the fact that the tunnel excavation below the Nala area and the bridge would start from neutral station, additional support measures are required for strengthening the soil (in front of the launching area) during the TBMs entrance in the ground, since at this stage there will not be adequate support pressure. Therefore, fully grouted self-drilling bolts 14 m in length 32 mm in diameter are foreseen to be installed perpendicular to the face wall of the neutral station, around the tunnel excavation area (**Figure 26**). The respective support measures have been also simulated in the respective 3D analysis as illustrated in **Figure 26**.

The last simulation (CH) is related with the settlement analysis of Chandpole Gate during the TBM tunnel boring below the monument. Detailed 3D model prepared simulating the Gate's foundations and the sequential construction of the tunnels with the two TBM shields (**Figure 27**).

In all the 3D analyses, the exact geometry of the segments and the annular gap of the tail shield grouting were simulated as presented in **Figure 28**. The excavation simulation is sequential, and in each step certain actions are considered. The advance of the TBM can be simulated either by considering the total length of the shield (e.g., 9 m in length) as one excavation step or slower advance of the shield equal to one segment can also be considered in the simulation. In the first case, the total load cases can be reduced, and thus the calculation time can be significantly

Figure 28.
Typical 3D view (left) of segmental lining and grout for backfilling the annular gap simulation. Typical 3D view (right) of segmental lining (blue) and grout (red) applied on soil (white) [11, 12].

minimized. Both methods of simulating the TBM advancement will give reliable results. It is preferable in cases of critical underpasses (e.g., U1, U2, and CH) for the excavation step to follow each segment length. Therefore, in such cases the analysis can commence with an initial excavation step equal to the shield's length, and as the TBM simulation reaches the important structure, the excavation step is to be reduced and should follow the segment length.

In each excavation step simulation, the EPB mean support pressure (as calculated in part A of TID) is applied at the tunnel face. Around the shield the same pressure with the face can be applied either with a triangular distribution reaching zero value on the tail of the shield or uniformly up to the half-length of the shield. Both methods are feasible, and the designer can decide based on the abilities of the software that he uses. In the previous step (behind the excavation), green grout (a modulus of elasticity equal to 1 GPa or less can be used) to simulate the backfill on the annular gap is applied along with the segmental lining. Two steps behind, the grout mature is simulated by applying its final properties (modulus of elasticity equal to 10 GPa). There are also other methods to simulate the TBM excavation, for example, interface elements can be used in order to simulate the behavior of the shield gap or the annular gap around the segments. Those methods need advance modelling and increased computational time, which are more appropriate for academic research and are not common practice in the design industry, since there are many unknown parameters that need to be defined in order to assign the correct properties to the interface elements.

In order for the calculated surface settlements to reach equilibrium behind the shield, a minimum excavation simulation of total tunnel length equal to 5 x diameters is mandatory. For special cases additional excavation length may be required to be simulated. In **Table 8** the total simulated length of tunnel excavation is given for all the performed 3D analyses along with geometrical required information.

In all the 3D analyses performed (**Table 8**), the plastic zone width was calculated below 0.5–1.0 m (**Figure 29**). It is obvious that this value was expected as it was initially derived based on Massinas and Sakellariou solution [6].

As it is evident from the diagram in **Figure 30**, the simulated support pressure (P_{fdm}, black dotted line) in the FDM 3D analysis is within the lower range of the Massinas and Sakellariou support pressure. The higher the overburden, the higher the pressure required to support the tunnel excavation, following second-order polynomial curve (e.g., the equation of trendline is $y = 8.89x^2–0.4x + 5.67$). On the contrary, the calculation of the support pressure, based on the earth pressure at rest, follows, as expected, linear line that results to unrealistic values, the application of them can jeopardize the effective operation of the TBM.

Section	Nos of octahedral elements	Tunnel axial distance (m)	Tunnel excavation radius (mm)	Tunnel internal radius (mm)	Segment ring length (mm)	Ring thickness (mm)	Total excavation length simulated (m)
F1–F8	65,000	15.5	3320	2900	1500	280	45
J1–J3	70,000	16.0	3320	2900	1200	280	48
U1	150,000	15.5	3320	2900	1500	280	108
U2	120,000	15.5	3320	2900	1500	280	88.5
CH	70,000	14.5	3320	2900	1200	280	48

Table 8.
3D models simulation properties.

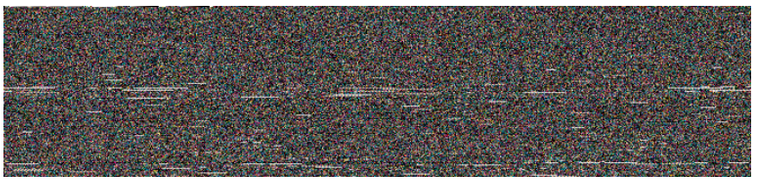

Figure 29.
Calculated plastic zone width (in red) as per TID of CC23 Delhi Metro (left) and as per TID of Jaipur Metro Phase 1b (right) [11, 12].

IntechOpen

IntechOpen

IntechOpen

Figure 30.
CC23 Delhi Metro. Calculated EPB support pressure for different overburden height as per critical sections F1–F8 of **Table 2** *and including the results from the 3D FDM analysis (P_{fdm}).*

Therefore, it is of greatest importance to avoid unnecessary conservatism when calculating the required TBM support pressure. The knowledge of the geotechnical conditions of the groundmass and the groundwater through proper established geotechnical campaign, in conjunction with the knowledge of the TBM operation principles, are the key factors for determining the required support pressure.

Following the establishment of the required support pressure in order to restrict the plastic zone formation width, the next step as per the TID is to evaluate the calculated induced surface settlements, in respect with the vulnerability of the existing surface and subsurface structures.

Following as example the CC23 Delhi Metro, the adopted support pressures in the 3D analyses resulted in minimum plastic zone widths in the order of 0.5–1.0 m and maximum surface settlements that are not exceeding 12 mm. After the total excavation of the two bores, the maximum calculated figures (independent of the overburden height) are bounded between 11 and 12 mm, as clearly illustrated in **Figure 31**.

It is evident that the range of maximum calculated surface settlements (7–11 mm) after the first bore excavation simulation is wider than the range calculated after both bore excavations. The overburden height is the key factor for this, and it is evident from the analyses results that the lower the overburden height, the greater the % of the developed surface settlements during the excavation of the first bore. As presented in the diagram of **Figure 32**, almost 90% of the total developed settlements are calculated during the first bore excavation for the shallowest case

Figure 31.
CC23 Delhi Metro. Maximum calculated surface settlements after first (left) and second (right) bore excavation simulations for sections F1–F8 of **Table 2** *(horizontal axis in m and vertical axis in mm).*

Figure 32.
CC23 Delhi Metro. Percentage of maximum developed surface settlements after first (left) bore excavation simulation for sections F1–F8 of **Table 2**. *Diagrammatic comparison of maximum calculated surface settlements after the first and second bore excavations (right).*

(11 m overburden), while for the deepest part of the alignment (25 m overburden), 60% of the total settlements are calculated (**Figure 32**). Of course the two bores' axial distance is another parameter which affects the surface settlements development range, but for shallow tunnelling in Metro projects, optimum value for the dimensionless ratio of the tunnels' axial distance to the diameter of the tunnel varies between 2.2 and 2.5. Even greater values than 2.5 can be applied, but it is economically preferable to keep the above range for the following reasons:

- Reduces the tunnel influence zone width, thus the surface monitoring is applied to less area.
- In case that the alignment does not permit reduction on the bores' axial distance before entering the station, results in wider station island platform.
- In case that the tunnel alignment permits the axial distance reduction before entering the station, additional complication is added in TBM alignment survey and navigation.

As it is evident from **Figure 32** (right), the projected maximum calculated surface settlements from first bore excavation, in respect to the different overburden heights, follow an exponential fit curve bounded by extreme values of 7 and 11 mm. With the proposed and simulated range of support pressure (0.8–1.5 bar), the totalv maximum calculated settlements after the excavation of the second bore follows a much steeper exponential fit curve bounded between 11 and 12 mm.

Further analysis of the curves of **Figure 32** (right), using the Gaussian formulae

$$S = S_{max}\, exp\left(\frac{-y^2}{2i^2}\right) = \frac{V_L}{i\sqrt{2\pi}}\, exp\left(\frac{-y^2}{2i^2}\right) \quad (1)$$

to calculate the surface settlements through the volume loss and the constant K, give results that are in good agreement with the 3D FDM, considering volume loss per bore equal to 0.6% for all the different overburden heights. Thus, proper calculation of the support pressure range controls the surface settlements and can lead to the same volume loss across the alignment independent of the overburden height.

The analysis of section CH (Chandpole Gate underpass) is another example to discuss the surface settlement development. Following the simulation of the support pressure as derived by Massinas and Sakellariou solution [6], the maximum 3D FDM calculated surface settlements are given in **Figure 33**.

DOI: http://dx.doi.org/10.5772/intechopen.90182

IntechOpen

Figure 33.
Jaipur Metro Phase 1b. 3D FDM calculated surface settlements after the first and second bore excavation simulations versus actual final monitored surface settlements [8].

After the first bore excavation simulation, the maximum surface settlement is calculated as 5 mm, while the second bore excavation only increases the surface settlement to 4 mm above the second bore without giving rise to the total maximum settlements. As already discussed in **Figure 32** (left), the shallow depth can give rise to the absolute maximum value of the surface settlements after the first bore excavation. The section CH, which is a case with extreme low overburden height, shows that even 100% of the final value of the surface settlements can be developed only during the first bore excavation, while the second tunnel construction can extend only the shape of the settlement trough without increasing the absolute maximum value. This is also visible from the actual monitored results; thus after the first bore construction (**Figure 34**), the maximum measured settlements at the Gate area are 6 mm, while after the second TBM underpass (**Figure 33**), only extent of the trough above its axis is measured, with absolute maximum value of the settlements equal to 2 mm.

Indeed, the application of the design support pressure (**Figure 35**—left) during the construction is the key factor along with the adequate tail shield grouting, in order to control the soil's settlements; the secret is to keep the chamber pressure constant in each stroke of the TBM, thus in each excavation step as the shield is moving forward (**Figure 35**—right).

To understand how the earth pressure is properly applied in the excavation chamber, the respective plots during the calibration of the TBM 1 are given in **Figure 36**. As it can be seen from the left diagram of **Figure 36**, during the calibration stage, the pressure drops at the beginning of the excavation for the construction of ring 78. This means that the chamber pressure during the last stroke of the previous ring 77 is not kept constant and as per the design requirements.

Therefore, at the beginning of ring 78 excavation, the support pressure inside the chamber is zero, and only after the excavation advanced 250 mm the pressure starts to rise. After the calibration stage, the support pressure inside the excavation chamber (**Figure 35**, right; and **Figure 36**, right) is kept constant along the entire excavation length. Along the calibration area, the maximum measured surface settlements were in the order of 10–14 mm. During the excavation simulation of the first tunnel, the maximum calculated deflection of the Gate's foundation (above the tunnel) is 1/1300, while the maximum differential settlement between the two foundations of the Gate is calculated 5 mm with an angular distortion of 1/1200.

Figure 34.
Jaipur Metro Phase 1b. Variation of measured surface settlements below the Gate for various relative positions of the first TBM (1) versus the final surface settlement along the Gate (left) and snapshot of recorded settlement values for cutterhead at ring position 110 (approx. 20 m, i.e., 3D ahead of the Gate) [8].

Figure 35.
Jaipur Metro Phase 1b. Variation of average face pressure per ring excavation versus the design range (as per section CH analysis), for TBM 1 (up line) and TBM 2 (down line) (left) [8].

Figure 36.
Jaipur Metro Phase 1b. Variation of face pressure of middle sensors along excavation of last ring of calibration drive (left) and first ring under the Gate (right) vs. the machine stroke [8].

Along the alignment of Jaipur Metro (3D FDM analysis J1–J3 as per **Table 7**), the maximum calculated surface settlements are in the order of 9–10 mm (**Figure 37**). As it is evident from **Figures 23** and **37**, all the buildings along the alignment are at 8 m distance from the tunnel bore axis. No structures are aligned above the tunnel centerline (except Chandpole Gate). Therefore, at the building location, the maximum calculated surface settlements are 4–5 mm. Maximum differential settlements are calculated 2 mm with an angular distortion of 1/2000.

For the case U1 of CC23 Delhi Metro, two analyses were performed. The first (as presented) includes the station structure, while the second is also performed without simulating the station. The purpose of the second analysis is to examine the effect of the station's stiffness on the development of the surface settlements. The presence of the stiffness of the existing tunnels and the Hauz Khas station affects the magnitude and the shape of the calculated surface settlements. In the first case, where the station is not simulated, the stiffness of the existing tunnels (Yellow Line) contributes to the development of the surface settlements by reducing their magnitude of approx. 10–15%.

This is evident in the diagram of **Figure 38** (left), where the maximum calculated surface settlements which are 30 m before the Yellow Metro Line is approx. 5 and 9 mm after the first and second bore excavations, respectively, while at a section just above and parallel with the up line axis of the Yellow Line, the surface settlements are calculated 4.5 and 8 mm, respectively. Therefore, a vertical shift on the settlement trough is observed, due to the stiffness of the existing tunnels, without affecting the overall shape of the trough but only the maximum value on

Figure 37.
Jaipur Metro Phase 1b. 3D FDM calculated surface settlements after total excavation of both bores (values in meters) (left). Projected maximum calculated surface settlements along tunnel alignment (right).

the settlement curve. On the other examined case, the simulation of the station has a more clear influence on both the shape and the magnitude of the surface settlements. As it is evident from **Figure 38** (right), both vertical and horizontal shift of the settlements curve is observed. The vertical shift is affecting the magnitude of the maximum calculated settlements which is in the order of approx. 3 and 6 mm after the first and second bore excavations, respectively. Thus, a reduction of approx. 30–40% is observed from the maximum values (5 and 9 mm) of the surface settlements. After the first bore underpass simulation, vertical displacements are calculated at the crown of the existing tunnels, with maximum values within the range of 3 and 5 mm (for both examined cases). After the second bore excavation, a slight increase on the crown vertical displacements is calculated, and the final maximum values are in the order of 7 and 8.5 mm (for the cases with and without station simulation, respectively). Again, the stiffness of the simulated station reduces the actual values of the crown displacements by producing vertical and horizontal eccentricity in the calculated curves, almost in the same degree as in the surface settlements which are presented before.

The maximum vertical displacements at the invert of the existing tunnels are calculated within the range of 3.5 mm (case with no station) and 6 mm (case with station) after the first bore excavation, with a maximum angular distortion in the order of 0.25‰ (no station simulation) having a peak value of 0.3‰ (station simulated) at the area which is in close vicinity with the station.

The advance of the second bore below the existing tunnels increases the invert displacements to 7 mm for the case where the station has been simulated and to 8.5 mm at the second case without the station been simulated, as it is evident in **Figure 39**. An increase on the differential displacements is also calculated with a maximum slope value reaching 0.4‰ (**Figure 40**). To sum up, for the case of U1 section, the maximum vertical displacements at the crown and the invert of the existing tunnels are calculated within the range of 3.5–6 mm with a maximum angular distortion of 0.3–0.35‰, after the first bore excavation simulation. The completion of the second bore excavation simulation gives rise to maximum vertical displacements at crown and invert equal to 7 and 8.5 mm, respectively, with a maximum angular distortion reaching the value of 0.4‰. The maximum horizontal displacements are calculated lower than 1 mm. The most critical aspect in U1 underpass is the execution of works with the existing tunnels under operation. Therefore minimum required displacements and differential settlements are acceptable at the track slab of the under operation tunnels. Details will be presented in the following chapter.

The case U2 of CC23 Delhi Metro was another critical underpass since in close vicinity with the tunnel launching shaft was the existing bridge and the water canal. The plastic zone width as it is evident in **Figure 41** is calculated less than 0.5 m width.

Figure 38.
Calculated surface settlements (m) at sections along the existing yellow line and 30 m before—case without station simulation in the left diagram and case with station simulation in the right diagram.

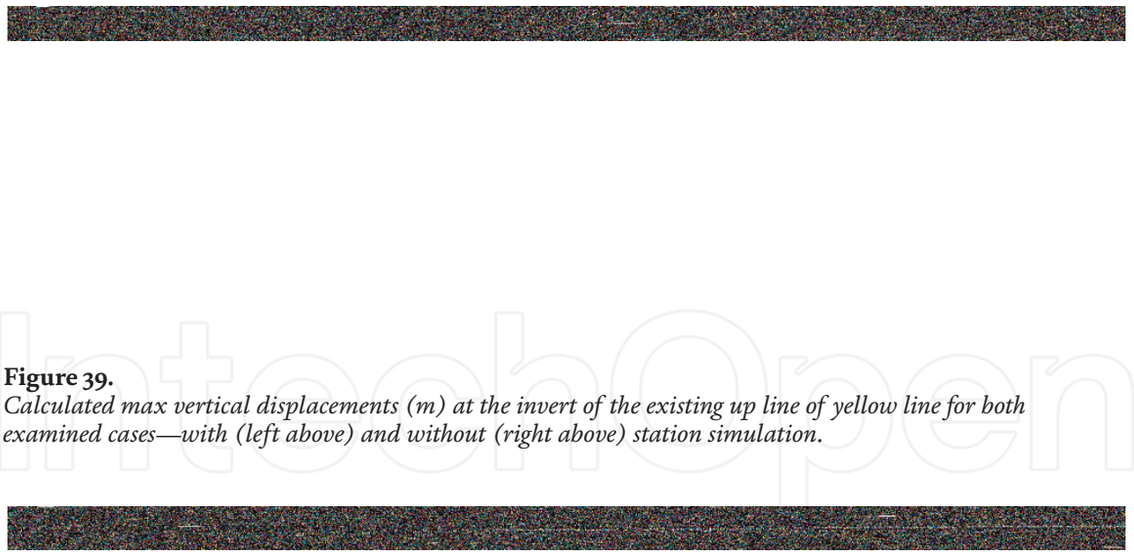

Figure 39.
Calculated max vertical displacements (m) at the invert of the existing up line of yellow line for both examined cases—with (left above) and without (right above) station simulation.

Figure 40.
Calculated max differential displacements at the invert of the existing up line of yellow line for both examined cases.

The maximum calculated surface settlements are in the order of 8–9 mm with a maximum deflection of 1/1000. At the area of the existing bridge, the surface settlements and angular distortion are calculated 2–8 mm and 1/1000, respectively. At the foundation level of the bridge (~4 m above tunnels crown), the maximum calculated vertical subsurface displacements are 10 mm with maximum angular distortion of 1/700 (**Figure 42**).

3.3.3 Part C: building risk assessment

The permissible settlements and deflections in structures are commonly assigned according to their vulnerability which is the output from the precondition survey.

The relation between the categories of damage and the vulnerability index is given by Chiriotti et al. [16] in **Table 9**. Considering the results from part B of TID, the conclusive **Table 10** is prepared in order to be used in correlation with **Table 9**.

Following **Tables 9** and **10**, for all sections F1–F8 of CC23 Delhi Metro, the buildings within the tunnel influence area are expected with "Negligible" damage. Furthermore, for Jaipur Metro Phase 1b, all the buildings are not aligned above the tunnel centerline (except Chandpole Gate). For those cases, the derived results show also "Negligible" damage category even if the existing old buildings of "Pink City" will be categorized as "Highly" vulnerable. Considering that Chandpole Gate vulnerability is in category "Slight," according to the precondition survey, "Negligible" damage is expected for settlements <6.7 mm and angular distortion <1/750. As already derived from the 3D analysis, the maximum calculated settlements and angular distortion are 5 mm and 1/1200, respectively, values which are

DOI: http://dx.doi.org/10.5772/intechopen.90182

Figure 41.
Calculated plastic zone width (left) and surface settlements (right) for case U2 of CC23 Delhi Metro [10].

IntechOpen

Figure 42.
Calculated surface settlements (left) and vertical displacements at the bridge's foundation depth (right), for case U2.

Damage category	Negligible		Low		Slight		Medium		High	
	0 < Iv < 20		20 < Iv < 40		40 < Iv < 60		60 < Iv < 80		80 < Iv < 100	
	Fr = 1.0		Fr = 1.25		Fr = 1.50		Fr = 1.75		Fr = 2.0	
	Smax (mm)	βmax	Smax (mm)	βmax	Smax (mm)	βmax	Smax (mm)	βmax	Smax (mm)	βmax
Negligible	<10	<1/500	<8	<1/625	<6.7	<1/750	<5.7	<1/875	<5	<1/1000
Slight	10–50	1/500–1/200	8–40	1/625–1/250	6.7–33	1/750–1/300	5.7–28.5	1/875–1/350	5–25	1/1000–1/400
Moderate	50–75	1/200–1/50	40–60	1/250–1/63	33–50	1/300–1/75	28.5–43	1/350–1/88	25–37.5	1/400–1/100
Severe	>75	>1/50	>60	>1/63	>50	>1/75	>43	>1/84	>37.5	>1/100

Table 9.
Relation between buildings' categories of damage and vulnerability index.

related with "Negligible" damage even in the case of "Highly" vulnerable structures. For the case of the bridge (U2), "Negligible" damage category is expected as per the calculated results presented synoptically in **Table 10**.

Following the damage assessment of the buildings within the influence zone of the tunnels, the trigger and alarm levels are mandatory to be established in order to monitor the actual the surface settlements and compare them with the calculated ones. Examples from real established trigger and alarm levels are given in **Table 11** for the critical sections U1, U2, and CH.

Concluding, the derived support pressures as per part A of TID resulted in acceptable surface settlements (calculated in part B), and consequently the building risk assessment (part C) proved that no additional measures are required to be

Section	Overburden (m)	Support pressure (bar)	Smax (mm)	βmax
F1	25	1.5	11	1/2500
F2	22	1.4	11	1/2500
F3	19	1.2	11	1/1700
F4	17	1.1	11	1/1650
F5	15	1.0	11	1/1450
F6	13	0.8	12	1/1250
F7	12	0.8	12	1/1050
F8	11	0.8	12	1/1000
U1	Existing tunnel invert at 4.5 m	1.8	8 (at existing tunnel invert)	1/2500 (at existing tunnel invert)
U2	Bridge at 4 m	1.5	10	1/700
J1	7	1.1	9 (3 at building area)	1/2000 (at building area)
J2	10	1.4	10 (4 at building area)	1/1500 (at building area)
J3	12	1.5	10 (5 at building area)	1/1500 (at building area)
CH	Chandpole Gate/4.5	1.5	5	1/1200

Table 10.
Synoptic presentation of calculated surface settlements.

Section	Measurement	Trigger level	Alarm level	Limit values
U1	Deflection of track slab of existing tunnels	±3 mm with gradient 0.20‰	±4 mm with gradient 0.25‰	±5 mm with gradient 0.3‰
	Displacement of existing tunnels' segmental lining	±4 mm	±6 mm	±8 mm
U2	Settlements at bridge area	7 mm	9 mm	10 mm
	Angular distortion	1/1000	1/777	1/700
CH	Settlements	4 mm	5 mm	6 mm
	Angular distortion	1/1400	1/1200	1/1000

Table 11.
Established trigger and alarm levels for sections U1, U2, and CH.

taken, in order to protect the existing surface and subsurface structures which are within the influence zone of the Metro tunnels.

4. Deep tunnelling in squeezing conditions

As presented in the previous paragraphs, shallow tunnel design is mainly related with the control of the induced surface settlement, in order to protect the existing surface and subsurface structures (monuments, important buildings, tunnels, bridges, etc.), and this can be achieved by minimizing the plastic zone width around the cavity. On the other hand, for the case of deep tunnels, excavated in difficult geological-geotechnical conditions, the aim is to design the tunnel excavation and primary support by allowing the ground mass to get plasticized and redistribute the stresses around the cavity but at the same time to control the extent of the plastic zone in order to achieve equilibrium in each excavation stage. The excavation of the tunnel is a dynamic phenomenon, since the development of the ground displacement is taking place ahead of the excavation face (~ half to one tunnel diameter) and reaches its maximum value about one- and one-half tunnel diameters behind the excavation face. Whether or not the above deformations induce stability problems in the tunnel depends upon the ratio of ground mass strength (σ_{cm}) to the in situ stress (P_o) level (**Figure 43**).

Figure 43.
Approximate relationship between strain and the degree of difficulty associated with tunnelling through squeezing rock, for unsupported tunnels [17].

Figure 44.
Comparison between rigid (red line) and yielding (blue line) support [18].

As it is evident from the curve of **Figure 43**, the smaller the ratio σ_{cm}/P_o, the higher the strain, and thus critical in the tunnel design is the control of the rock mass deformations around the cavity. Therefore, in case of deep tunnels with high overburden and low rock mass properties, controlled plasticization is almost mandatory in order to reduce the exerted loads around the excavation. By intervening with application of proper yielding support measures, the rock mass is deformed plastically under controllable manner. This solution involves the introduction of deformable elements into the lining. These elements are allowed to deform by a predetermined amount, and when this limit is reached, the support system becomes rigid and starts to carry the full support load. This process allows progressive failure to occur, and a plastic zone is formed in the rock mass immediately surrounding the tunnel. This progressive failure results in a redistribution of the stresses in the rock, surrounding the tunnel, and in a significant reduction in the capacity of the support system required to stabilize the tunnel.

The concept is illustrated in **Figure 44**. Different behavior patterns of rigid (red line) and yielding (blue line) supports are compared. As the rigid support system is installed at a roof displacement of 100 mm, the rock mass loads are that high that the system fails. On the other hand, when a flexible yield support is installed at the same initial crown displacement (100 mm), the controllable deformation of the rock (to 300 mm) through the yielding joints reduces the loads transferred to the support after "locking" of the sliding joints (**Figure 44**, right), without failure of the system.

In the following paragraphs the case study from one of the most difficult tunnels around the world will be analyzed, and details from the design of critical sections will be presented.

4.1 Yacambu-Quibor tunnel overview

A characteristic example of a deep tunnel case, where excessive loads and deformations are recorded around the excavation, is the Yacambu-Quibor tunnel in Venezuela. The 26.4-km-long tunnel (**Figure 45**) was originally conceived as an unlined TBM-driven tunnel to convey water from the Yacambu dam in the wet Orinoco River basin to the dry agricultural region around Quibor. Construction commenced in 1976 in anticipation that the majority of the rock mass through which the tunnel would be driven would be silicified phyllite. This rock forms very steep and stable cliffs in the area of the dam site, and numerous unsupported exploration and drainage tunnels have remained stable for many years in the dam abutments. Unfortunately, it soon became apparent that the rock mass through which the tunnel had to be driven is composed largely of graphitic phyllite which, in contrast to the silicified phyllite of the dam site, is a very weak and tectonically disturbed material. Unsupported tunnels cannot be driven in this rock, particularly at the cover depths of up to 1200 m that occur in the center of the tunnel. In addition, the Bocono fault and the Turbio fault had to be crossed by the tunnel, and it was anticipated that these would cause significant stability problems. Floor heave in the original TBM-driven tunnel resulted in abandoning the tunnel in 1979, and all subsequent tunnel driving decided to proceed with conventional drill and blast and mechanical excavation. Steel sets embedded in a shotcrete lining provided the main support system with the use of forepoling, spiling, and rockbolting where required. Spalling of the shotcrete lining and floor heave has continued as problems whenever the rock mass deformation has been more severe than anticipated.

During the driving of the Ventana Inclinada (**Figure 45**), an intermediate access tunnel designed to provide early access to the Bocono Fault, severe squeezing was encountered. This is a phenomenon characterized by closure of the tunnel, and it

DOI: http://dx.doi.org/10.5772/intechopen.90182

IntechOpen

IntechOpen

Figure 45.
Yacambu-Quibor tunnel longitudinal section [18].

occurs when the rock mass surrounding the tunnel is overstressed and a "plastic zone" develops, as described previously. Unless adequate support measures are introduced, this squeezing can develop into uncontrolled closure and eventually collapse of the tunnel. The primary cause of squeezing is, as already described, a combination of a weak rock mass subjected to high in situ stresses due to a high overburden cover. The process is exacerbated by the presence of water and by gradual deterioration or "creep" of the rock mass.

4.2 Graphitic phyllite

In the case of the graphitic phyllite, shown at the Salida heading in **Figure 46**, the tectonically disturbed rock mass makes it very difficult to collect samples for laboratory testing, and, consequently, very little reliable rock mass strength data is available.

The choice of an appropriate intact strength from results such as those presented in **Figure 46** is a highly subjective process. Anisotropic and foliated rocks such as slates, schists, and phyllites, whose behavior is dominated by closely spaced planes of weakness, cleavage, or schistosity, present particular difficulties in the determination of the uniaxial compressive strengths. Salcedo has reported the results of a set of directional uniaxial compressive tests on a graphitic phyllite from Venezuela. It will be noted that the uniaxial compressive strength of this material varies by a factor of about 5, depending upon the direction of loading. Evidence of the behavior of this graphitic phyllite in the field suggests that the rock mass properties are dependent upon the strength parallel to schistosity rather than that normal to it. In the case of Yacambu-Quibor, the many years of experience of the behavior of the tunnel gives adequate information to calibrate the rock mass strength to a certain degree. It is recommended that the parameter that should be varied in this calibration is the intact rock strength σ_{ci} since this is both logical from a mechanics point of view and it has a very significant numerical influence on the estimated rock mass strength. For the good siliceous phyllites, the intact rock strength σ_{ci} was determined as 40–50 MPa, while for the more carbonaceous and foliated phyllites (graphitic phyllite), the intact rock strength varies from 15 to 30 MPa.

Approximately 5 km of tunnel remained to be excavated, and it is anticipated that a significant portion of this length will be in graphitic phyllite and that this will be under the high overburden cover (up to 1200 m). The Turbio fault, which is clearly defined on surface, may extend to tunnel depth, and provision had to be made for

Figure 46.
Tectonically deformed graphitic phyllite exposed in excavated face of Salida heading of Yacambu-Quibor tunnel on 24 November 2003 (left) and influence of loading direction on strength of graphitic phyllite (right) [18].

excavating through and stabilizing the tunnel in this fault. It is also possible that high pressure water and methane gas could be encountered in excavating through the Turbio fault. Therefore, for designing the remaining un-excavated part (approx. 5 km), the information from two critical stations at KP 6+540 and KP 11+700 along the excavated tunnel (**Figure 47**) were used in order to design the most adequate support measures and excavation profile as well as the final lining of the tunnel.

4.3 Support types

The support types along the tunnel were divided into two main categories. Three full face horseshoe types S1, S2 and S3 for their application in silicified phyllite with GSI values greater than 50 (Rock mass types A, B and C) were foreseen, for fault zones and areas with large intrusions of graphitic phyllite at the excavation face (Rock mass types D1 and D2) with GSI values even low to 25 (**Figure 48**).

The flexible support types (S4 and S5) consist of shotcrete with total final thickness up to 60 cm (to act also as final lining), steel sets with sliding joints embedded in the shotcrete lining placed in axial distances of 0.6–1.0 m, and 10–12 fully grouted rock bolts installed every round length. Two sliding joints were foreseen for class S4 at the vaulted area (**Figure 49**), while three flexible joints were equally spaced in category S5. In both flexible support classes, the sliding joints gap was 30 cm as shown in the detail of **Figure 49**.

4.4 Tunnel station at KP 11+700

In order to investigate the behavior of the tunnel and the reaction of the flexible support class, to be used in the Turbio fault area, the particular case of the support near station 11+700 in the Salida heading was considered, and detailed 3D FEM analysis is elaborated. Near the station the conditions were as follows:

Rock mass classification: GSI 35
Tunnel cover: 1100 m
Horizontal-vertical stress ratio (K_o): 1.15
Assumed radial deformation before final closing: 300–350 mm

An intact rock strength of 20 MPa is considered, and the following rock mass properties are considered in the simulation:

- Unit weight, γ (kN/m^3): 25
- Cohesion, c (MPa): 1.28
- Friction angle, φ (°): 19.72
- Young modulus, E (MPa): 1905
- Poisson ratio, ν: 0.30
- Rock mass strength, σ_{cm}: 2.4 MPa

It is well noticed that the ratio σ_{cm}/P_o (<0.1) for the above case reveals extreme squeezing conditions. Following the above, support type S4 has been examined. For the simulation, SOFiSTiK [19] software was used. Large model is constructed

Figure 47.
Geological-geotechnical section of Yacambu-Quibor tunnel [18].

IntechOpen

IntechOpen

DOI: http://dx.doi.org/10.5772/intechopen.90182

IntechOpen

IntechOpen

Figure 48.
Support types of Yacambu-Quibor tunnel [18].

Figure 49.
Support type S4 with sliding joint detail and photos [18].

DOI: http://dx.doi.org/10.5772/intechopen.90182

Figure 50.
3D finite element model of Yacambu-Quibor tunnel temporary support with sliding joints and roof displacement (ratio) versus tunnel advance [18].

consisted of octahedral brick elements. An excavation diameter of 5.2 m is simulated with application of shotcrete shell, simulated with quadrilateral 4-noded elements. For the simulation of sliding joints, spring elements were used with closure gap of 300 mm. Excavation length is considered 1.5 m. Typical view of the 3D model is presented in **Figure 50** (left).

The 3D analysis results (**Figure 50** right) showed that the crown vertical displacement of the rock begins approximately one diameter ahead of the tunnel face and reaches its maximum value about one- and one-half tunnel diameters behind the excavation face.

The total crown vertical displacement is calculated in the order of 200 mm. It is noted that the 200 mm gap closure gives a crown vertical displacement equal to ~60 mm for a tunnel radius equal to 2.6 m, while for the same radius but for a total closure of 300 mm, the crown displacement is calculated 100 mm.

Since the 3D modelling requires enormous computational time, due to large strain conditions, 2D FEM models were also constructed, and further parametric analysis was executed in order to confirm the findings from the previous 3D analysis. Using the convergence-confinement method (Panet 1995), for an unsupported deep tunnel, to assess the rock mass displacement ahead of the excavation face, two cases were investigated. In the first FEM model (S4–1), detailed simulation technique of the sliding joint closure is considered using spring elements. In the alternative FEM model (S4–4), a more simplified approach was used. The principle of the flexible support is that during the movement of the sliding joints, the stresses are released from the shotcrete shell, and only after the total closure of the joints, the temporary shell starts to carry the rock mass loads. Considering this principle, the support system (shotcrete shell) is activated when the crown displacement reaches the value which includes also the locking of the joints, thus rock mass displacement ahead of the face plus additional vertical movement due to joint gap closure. In **Figure 51**, the simulation steps for the two models are presented.

Considering the convergence-confinement method, a crown displacement equal to 150–200 mm is calculated 2–3 m ahead of the excavation face. In model S4–1 the resulted relaxation as per the convergence-confinement method is considered in LC1, and the respective relaxation value is applied on the face core. As per the analysis results, this led to a crown displacement of 211 mm, thus is matching the convergence-confinement calculations. Following the simulation of the sliding joints, at the end of LC2, the spring displacement (gap closure) is calculated 320 mm and the crown displacement equal to 305 mm. After the final excavation of the tunnel, simulated in LC3, the total crown displacement is calculated 315 mm. For the case of model S4–4, a total relaxation is considered in order to simulate the rock mass relaxation ahead of the tunnel face plus the

Figure 51.
Simulation stages for S4–1 model (left) and S4–4 model (right) [20].

Location	Crown vertical displacement (mm) for S4–1/S4–4	Sliding joint closure (mm) for S4–1/S4–4	Shotcrete shell axial force (kN) for S4–1/S4–4
2–3 m ahead of excavation face	211/indirectly simulated	NA	NA
2–3 m behind excavation face	305/304	320/indirectly simulated closure of 300	6500/indirectly simulated
Final excavation with 60 cm final shotcrete thickness	315/309	NA	9000/8500

Table 12.
Simulation results from 2D models S4–1 and S4–4.

closure of the sliding joints. Therefore, a value of 300 mm is considered in LC1 at the crown area, followed by a value of 308 and 309 mm at the end of LC2 and LC3, respectively. In both simulations the maximum axial force on the shotcrete shell is calculated after the total closure of the sliding joints, followed by the total excavation of the tunnel; 8500–9000 kN is calculated in model S4–1, while in S4–4 a maximum value of 8000–8500 kN is derived. In **Table 12** the results from both analyses are presented.

For tunnelling in extreme squeezing conditions, it is preferable for the parametric design to be performed with 2D FEM or FDM computational analysis models. Parametric analysis is mandatory in such cases, to examine the behavior of the tunnel for a range of the rock mass properties, since a small change in the intact rock strength or the overburden height or the GSI value can lead to different results. 2D FEM parametric modelling is quicker and, with the guidance provided herein, can lead to proper dimensioning of the required support measures. Of course, 3D FEM analysis can be used as additional to the 2D calculations in order to examine the longitudinal development of the displacements.

Following the results presented above, the S4 support class with 60 cm of shotcrete shell (which will be used as the permanent lining of the tunnel) and two sliding joints with 300 mm gap closure (**Figure 52**) proved adequate to be used for the un-excavated part of the tunnel. Further analysis of the results shows that possible reduction also on the final shotcrete shell thickness to 50 cm was also adequate, while 40 cm can also be utilized in special cases where the closure of the sliding joints was not fully mobilized (evidencing better rock conditions).

4.5 Tunnel station at KP 6+540

Another also critical case that was mandatory to be examined in order to conclude on the support measures to be used for the un-excavated part was the findings near station KP 6+540 in the Entrada heading where a failure event was occurred.

After station 6+487, tunnel conditions were of GSI 50, 1225 m cover, and almost no ground deformation. For this situation a support type S3 (horseshoe) with 25 cm of shotcrete thickness was being used. In station 6+540 a tunnel slide occurred and was evaluated as a fault zone. While a geological, geotechnical, and support evaluation was in progress toward a heavier support, the contractor proceeded to place four steel ribs without sliding joints in S3 horseshoe geometry with 4.60 m excavation diameter. The measured deformations in sections before and after the main slide were of the order of 45 cm.

Figure 52.
S4 support class with 60 cm shotcrete thickness for station KP 11+700 [18].

The recommended excavation and support classes, according to Yacambu tunnel experience were:

- In the area of the fault zone, support type S4 with 40 cm of shotcrete in horseshoe geometry with 4.60 m diameter (minimum internal diameter of 3.80 m).

- In the area before and after the fault zone, support type S4 in circular geometry.

The type S4 (horseshoe and circular geometry) has been examined in detail in this paragraph by 2D finite element analysis in order to investigate the implementation of type S4 section (horseshoe and circular geometry) during the long-term operation of the project as well as to use the findings for the un-excavated part of the tunnel.

Considering the event near the station KP 6+540, the conditions were considered as follows:

Rock mass classification: GSI 25
Tunnel cover: 1200 m
Horizontal-vertical stress ratio (K_o): 1.0

An intact rock strength of 15 MPa is considered, and the following rock mass properties are adopted in the simulations:

- Unit weight, γ (kN/m^3): 25

- Cohesion, c (MPa): 0.963

- Friction angle, φ (°): 16.12

- Young modulus, E (MPa): 918

- Poisson ratio, ν: 0.30

- Rock mass strength, σ_{cm}: 1.4 MPa

4.5.1 Simulation stages in the area of the fault zone

Using the convergence-confinement method (i.e., Panet) and elastoplastic response with Mohr-Coulomb law, the displacements 3–4 m ahead of the tunnel face are estimated 50–30 cm (see **Figure 53**).

Thus, before the tunnel sliding, the radial displacement is estimated about 30–50 cm. After the event, which happened in station 6+540 (tunnel slide) and was evaluated as a fault zone, additional displacements (45 cm), in sections before and after the main slide, were measured.

Considering the additional displacements (45 cm) due to the tunnel sliding as well as the radial displacements (30–35 cm) before the event, the total radial displacements in the area before and after the fault zone are estimated at about 75–80 cm. In the area of the fault zone, where the tunnel slid, the total radial deformations are estimated higher, about 80–100 cm. Following the above, four (4) 2D models are prepared using software SOFiSTiK [19] in order to check the adequacy of the shotcrete shell, as follows (**Table 13**).

IntechOpen

Figure 53.
Inward radial displacement as per convergence-confinement method for unsupported tunnel [21].

Model	Initial rock displacement considered (mm)	Tunnel profile	Diameter (m)	Shotcrete thickness (cm)
S4a–c	450	Circular	4.6	50
S4b–c	800	Circular	4.6	50
S4b–h	800	Horseshoe	4.6	40 crown 60 invert
S4c–h	1000	Horseshoe	4.6	40 crown 60 invert

Table 13.
2D FEM analysis for tunnel station KP 6+540.

IntechOpen

Figure 54.
Modulus of elasticity reduction as per convergence-confinement method [21].

The initial rock deformations 45 cm (S4a–c), 80 cm (S4b–c, S4b–h), and 100 cm (S4c–h) are investigated in Load Case LC1, by considering an initial reduction in elasticity modulus of the core of the order of 98% (45 cm), 99.3% (80 cm), and 99.5% (100 cm), respectively, as per Panet curves. In the next step, the installation of a temporary support shell with minimum stiffness is simulated

(10 cm shotcrete in tunnel periphery) with further reduction in elasticity modulus of the core (as it is presented in **Figure 54**) (Load Case LC2).

According to the tunnel construction sequence, fully cemented rock bolts (with diam. 25 mm up to 35 mm) are implemented in the previously erected steel set. Additional thickness of temporary support shell (5 cm) is simulated with further reduction in elasticity modulus of the core. Shotcrete thickness of 15 cm has reached its final strength (Load Case LC21). The simulation of excavation is fulfilled in Load Case LC3 by considering that the support measures will be mobilized 100% (full stiffening of the 50 cm shotcrete shell for S4a–c and S4b–c and of the 40 cm shotcrete shell in the crown and 60 cm in the invert for S4b–h and S4c–h). The produced stresses in the lining (by considering normal (N) and shear (V) forces, as well as bending moments (M)) are considered, and the appropriate radial and shear reinforcement is then calculated.

In a second step, the long-term behavior of the lining is investigated. A reduction of 15–20% of the rock mass properties is considered, and strain-softening material is used, as follows:

Young modulus, E = 918 MPa
Cohesion, c = 963 MPa
Friction angle, $\varphi = 16.12°$
Poisson ratio, $\nu = 0.3$
Plastic ultimate strain, $\varepsilon_u = 9.88‰$
Ultimate friction angle, $\varphi_u = 15.30°$
Ultimate cohesion, $c_u = 0.871$ MPa

Figure 55.
Model S4a–c and S4b–c, calculated plastic zone (top-left and bottom-left, respectively) and axial force (12,500 and 8500 kN, respectively) distribution (top-right and bottom-right, respectively) within the final shotcrete shell [21].

(Young modulus and ultimate shear strength are derived by the taken GSI = 25, mi = 10, and σ_{ci} = 15 MPa).

Load Case LC4 is used as a long-term behavior calculation step. The thickness of the final lining is reduced to 40 cm for S4a–c and S4b–c and to 35 cm for S4b-h and S4c-h due to the risk of weathering of the external shotcrete layer. Rockbolts are considered as not functional.

4.5.2 Result presentation

Four (4) different models have been elaborated in order to investigate the sensitivity of the reinforcement results (for the final lining of S4, in either a circular and a horseshoe geometry), in comparison with the initial rock mass deformation (45, 80, 100 cm) due to the tunnel sliding that occurred near station at KP 6+540. In all models the detailed construction sequence has been analyzed along with the respective initial rock mass deformation. In the first model S4a–c the initial rock mass convergence that is simulated, before the installation of the temporary support, is 45 cm.

At the second model (S4b–c), it is assumed that the reported deformation of 45 cm (ING-03-52) does not include initial deformation occurred before the slide (estimated of the order of 30–35 cm), and therefore the total deformation is of the order of 80 cm. The resultant axial forces, regarding the first approach, are higher than the axial forces that are calculated with the second model (**Figure 55**).

The second approach as mentioned above considers both convergences that are produced by (a) relaxation of the rock mass (30–35 cm) which is supposed to be occurred before the excavation and (b) additional measured displacement of the rock mass (before and after the fault zone) due to tunnel failure. The corresponding values of the axial and shear forces along with the moments that are developed in the flexible temporary lining is a result of the shell's displacement. Thus, the lower the displacement of the shell, the lower the axial and shear forces and moments. In a long-term basis, the stresses that were developed in the temporary lining are redistributed within the total thickness of the final lining. Considering the behavior of the tunnel near station 6+540, where no important shell displacements were occurred after the installation of the first 15 cm of shotcrete, it is assumed that the initial rock mass convergence before the installation of the shell was about 80 cm.

For models S4b–h and S4c–h, the radial initial displacement of the rock mass is estimated at about 80–100 cm, due to the fact that the area, which is investigated, is the fault zone, where the tunnel failed. The results for these analyses are unfavorable. In both approaches the bending moments and shear forces, in the connection area of the vault with the invert, are extremely higher than the previous model S4b–c (**Figure 56**).

Figure 56.
Model S4b–c, calculated plastic zone (left), axial force (9000 kN) distribution (middle), and bending moments (max 1300 kN m—right) within the final shotcrete shell [21].

DOI: http://dx.doi.org/10.5772/intechopen.90182

The reason for the unfavorable results is the "bad" geometry of the horseshoe support class (see **Figure 48**). Even in cases that further failure has not been observed in the areas of adjustment to KP 6+540, where the horseshoe geometry was applied, a decision had to be made in order to secure the tunnel lining on a long-term basis.

IntechOpen

Figure 57.
Calculated required reinforcement for long-term tunnel operation. Model S4b–c (left) with max 14 cm² and model S4b–h (right) with 43 cm² at crown and max 140 cm² [21].

IntechOpen

Figure 58.
Conversion of horseshoe tunnel excavation profile to equivalent circular final lining for long-term tunnel operation [21].

Station	KP 11+700	KP 6+540
Overburden height, H (m)	1100	1200
GSI	35	25
σ_{ci} (MPa)	20	15
Rock total radial closure (mm)	300–350	650–750
Sliding gap (mm)	2 × 300	3 × 300
Final lining axial force (kN)	8500	8500–12,500
Support class	S4	S5
Lining thickness (mm)	500	500–600

Table 14.
Support classes and application criteria for GSI 25–35.

From the detailed FEM analysis results, it was clear that a circular geometry for the final lining during the long-term operation of the tunnel was able to withstand the rock load with a minimum required reinforcement of 14 cm^2 (**Figure 57**), while the horseshoe geometry was unfavorably affecting the capacity of the final lining. Therefore, special reinforcement arrangement was applied in order to convert the tunnel excavation profile to an equivalent circular final lining (**Figure 58**).

4.6 Conclusive remarks for extreme squeezing conditions

The detailed analysis and back-analysis of the tunnel in the two critical stations at KP 11+700 and KP 6+540 describe the behavior of the excavation and consequently the support classes, under the worst geotechnical conditions which are governed by the presence of very weak carbonaceous and foliated phyllites (graphitic phyllite) with GSI <35 and intact rock strength from 15 to 30 MPa.

The tunnel excavation under maximum overburden height and in the presence of rock with GSI value of 35 and intact rock strength of 20 MPa can lead to a total radial closure of 300–350 mm. For the extreme case of GSI = 25 and σ_{ci} = 15 MPa, the total radial closure can be in the order of 650–750 mm. For both cases, the circular excavation profile of S4 and S5 support classes is suitable and needs to be implemented in order to secure the long-term operation of the final lining. **Table 14** summarizes the findings from the parametric analysis.

As it is shown in detail in the respective chapters, the tunnel excavation under extreme squeezing conditions is only feasible by applying a flexible support category with sliding joints in a circular excavation profile.

5. Conclusions

In the present chapter of the book, the shallow and deep tunnel cases are explained in detail, and methods of designing are presented. For the reader and the tunnel designer, the following conclusions are summarized for the shallow and deep tunnel problems.

5.1 Shallow tunnelling in urban environment

Knowledge of the general macro-geology of the project area is always beneficial for the designer to establish a proper geotechnical campaign.

The general geological formations of the under-study area will be the governing parameter for establishing the density of the investigation boreholes and the density and type of laboratory tests.

Knowledge of the geological-geotechnical conditions will determine the type of the TBM shield to be used as well as the cutterhead design.

Combination of analytic solutions and computational advance modelling (FEM or FDM) is the most adequate method to be used in the design, since it reduces the time required for executing the calculations.

TBM tunnel interstation design is mandatory to be followed in Metro projects, due to the existence of surface and subsurface structures. The aim of the design to control the surface settlements and thus the operation of the TBM shields need to be determined by the designer.

Conservatism in determining the geotechnical properties of the soil must be avoided since it will result in overdesigning the permanent segmental lining of the tunnel and will also lead to unreasonably high support pressures with immediate detrimental effect on the operation of the machine.

The discrete parts A, B, and C determined the TBM TID and as such need to be strictly followed.

The application of the design support pressure (as derived from the TID) is the key factor along with the adequate tail shield grouting, in order to control the soil's settlements. The adequate application is to keep the chamber pressure constant in each stroke of the TBM, thus in each excavation step, as the shield is moving forward. Grouting from the tail shield of the TBM must be performed, and the amount and pressure of grout injected into the annular gap must be controlled by the pilot of the machine, and the consumed volume must always be monitored per ring along with the applied grouting pressure. Grouting amount in general should be 1.1–1.2 times of the interspace cubage. Secondary grouting from the segments should be performed based always on the live monitoring data.

5.2 Deep tunnelling in extreme squeezing conditions

Anisotropic and foliated rocks such as graphitic phyllites, when met under high in situ pressure, can always lead to extreme squeezing problems.

For extreme squeezing conditions only, flexible supports can secure the stability of the underground excavation. Any other type of stiff support will result in failure.

Long-term behavior of weak rocks should always be investigated when permanent lining is designed.

The most adequate excavation profile is the circular geometry. Horseshoe geometries should be avoided since the resultant bending moments will lead to undesignable conditions. Larger tunnels (>5 m diameter) should be designed with a geometry as close as possible to a circle.

For larger tunnel diameters to be constructed in extreme squeezing conditions with increased number of sliding joints (or lining stress controllers (LSC)), 3D FEM or FDM computational analysis will be required with advance modelling of the sliding interface in order to investigate the closure sequence of the joints in relation to the advance of the tunnel face. Using the results from the 3D analysis, relaxation factors can be used in 2D modelling, and the temporary support measures dimensioning can be achieved.

Acknowledgements

I would like to express my gratitude to Omikron Kappa SA for the more than 17 years of continuous cooperation that we have in performing designs for

demanding and difficult projects around the globe. Special thanks also to Dr. Evert Hoek for his valuable guidance in my early years as a designer in the Yacambu-Quibor tunnel project.

To download the chapter with high resolution images, please use the following link: https://cdn.intechopen.com/public/docs/70605.pdf

IntechOpen

Author details

Spiros Massinas[1,2,3,4,5]

1 Engineering Manager of ALYSJ JV (Aktor - Larsen and Toubro - Yapi Merkezi - STFA - Al Jaber Engineering JV), Gold Line Metro, Doha, Qatar

2 Middle East and India Regional Manager of Omikron Kappa Consulting, Doha, Qatar

3 Project Manager/Director of Omikron Kappa – Indus Consultrans JV, Gurgaon, India

4 Civil Engineer, PhD (NTUA), MSc (NTUA), CEng (UK), MICE UK

5 Associate Researcher, Laboratory of Structural Mechanics, Department of Infrastructure and Rural Development, National Technical University of Athens (NTUA), Greece

*Address all correspondence to: spirosmas@yahoo.gr

IntechOpen

© 2019 The Author(s). Licensee IntechOpen. This chapter is distributed under the terms of the Creative Commons Attribution License (http://creativecommons.org/licenses/by/3.0), which permits unrestricted use, distribution, and reproduction in any medium, provided the original work is properly cited. CC BY

References

[1] Massinas S. Analytic solution for shallow tunneling problems in elastic-plastic half space [thesis]. National Technical University of Athens; 2019

[2] Bray JW. Some applications of elasticity theory. In: Brown ET, editor. Analytical and Computational Methods in Engineering Rock Mechanics. London: Allen & Unwin; 1987. pp. 32-94

[3] Omikron Kappa—Indus Consultrans JV. Geotechnical interpretation report for tunnels. CC23 Delhi Metro; 2013

[4] Omikron Kappa—Indus Consultrans JV. Geotechnical interpretation report for tunnels, stations and shafts. Jaipur Metro Phase 1B; 2014

[5] Anagnostou G, Kovari K. Face stability conditions with earth pressure balance shields. Tunnelling and Underground Space Technology. 1996;**9**:165-174

[6] Massinas S, Sakellariou M. Closed form solution for plastic zone formation around a circular tunnel in half space obeying Mohr-coulomb criterion. Geotechnique. 2009;**59**(8):691-701. DOI: 10.1680/geot.8.069

[7] Massinas S, Daljeet S, Saini MIS, Bhardwaj V, Aishwarya K. Settlement analysis and monitoring instrumentation of Delhi Metro's operational Line-2 tunnels during TBM of new Line-8 underpass. In: Proceedings of the ITA WTC 2015 Congress; 22-28 May 2015; Lacroma Valamar Congress Center, Dubrovnik, Croatia

[8] Massinas S, Prountzopoulos G, Bhardwaj V, Saxena A, Clark J, Sakellariou M. Design aspects of under-passing a city's heritage landmark with EPB machines under low overburden: The case of Chandpole Gate in Jaipur Metro, India. Geotechnical & Geological Engineering. 2018. DOI: 10.1007/s10706-018-0565-0

[9] FLAC3D, Fast Lagrangian Analysis of Continua in 3 Dimensions, Itasca Consulting Group, Inc. US Minneapolis. Available from: www.itascacg.com

[10] Omikron Kappa—Indus Consultrans JV. Design of under passing existing bridge at Nala area. CC23 Delhi Metro; 2013

[11] Omikron Kappa—Indus Consultrans JV. TBM tunnel interstation design—Assessment and protection of existing buildings. CC23 Delhi Metro; 2013

[12] Omikron Kappa—Indus Consultrans JV. TBM tunnel interstation design—Assessment and protection of existing buildings. Jaipur Metro Phase 1B; 2014

[13] Massinas S, Sakellariou M. A parametric study of tunneling-induced surface settlements under 3D conditions. In: Proceedings of 2nd International Conference "From Scientific Computing to Computational Engineering"; 5-8 July 2006; Athens, Greece

[14] Omikron Kappa—Indus Consultrans JV. Design of under passing existing mMetro line (yellow) near Hauz Khas—Stage 3 analysis. CC23 Delhi Metro; 2013

[15] Omikron Kappa—Indus Consultrans JV. Under passing scheme for Chandpole gGate. Jaipur Metro Phase 1B; 2014

[16] Chiriotti E, Marchionni V, Grasso P. Porto Light Metro System, Lines C, S and J. Compendium to the

Methodology Report on Building Risk Assessment Related to Tunnel Construction. Normetro – Transmetro. Italian, Portuguese: Internal Technical Report; 2000

[17] Hoek E, Marinos P. Predicting tunnel squeezing problems in weak heterogeneous rock masses. Tunnels and Tunnelling International. 2000;**32**(11):45-51

[18] Hoek E—Omikron Kappa Consulting Ltd. Yacambu-Quibor tunnel lining; 2003

[19] SOFiSTiK, Finite Element Method Software, Sofistik AG. Available from: www.sofistik.com

[20] Omikron Kappa Consulting Ltd. Excavation, temporary and final lining design for Yacambu-Quibor tunnel near station in KP 11+700; 2003

[21] Omikron Kappa Consulting Ltd. Excavation, temporary and final lining design for Yacambu-Quibor tunnel near station in KP 6+540; 2003

IntechOpen